

## Radiative effect of clouds on tropospheric chemistry in a global three-dimensional chemical transport model

Hongyu Liu,<sup>1</sup> James H. Crawford,<sup>2</sup> Robert B. Pierce,<sup>2</sup> Peter Norris,<sup>3,4</sup> Steven E. Platnick,<sup>3</sup> Gao Chen,<sup>2</sup> Jennifer A. Logan,<sup>5</sup> Robert M. Yantosca,<sup>5</sup> Mat J. Evans,<sup>5,6</sup> Chieko Kittaka,<sup>7</sup> Yan Feng,<sup>8,9</sup> and Xuexi Tie<sup>10</sup>

Received 23 June 2005; revised 30 January 2006; accepted 5 July 2006; published 18 October 2006.

[1] Clouds exert an important influence on tropospheric photochemistry through modification of solar radiation that determines photolysis frequencies (J-values). We assess the radiative effect of clouds on photolysis frequencies and key oxidants in the troposphere with a global three-dimensional (3-D) chemical transport model (GEOS-CHEM) driven by assimilated meteorological observations from the Goddard Earth Observing System data assimilation system (GEOS DAS) at the NASA Global Modeling and Assimilation Office (GMAO). We focus on the year of 2001 with the GEOS-3 meteorological observations. Photolysis frequencies are calculated using the Fast-J radiative transfer algorithm. The GEOS-3 global cloud optical depth and cloud fraction are evaluated and generally consistent with the satellite retrieval products from the Moderate Resolution Imaging Spectroradiometer (MODIS) and the International Satellite Cloud Climatology Project (ISCCP). Results using the linear assumption, which assumes linear scaling of cloud optical depth with cloud fraction in a grid box, show global mean OH concentrations generally increase by less than 6% because of the radiative effect of clouds. The OH distribution shows much larger changes (with maximum decrease of  $\sim 20\%$  near the surface), reflecting the opposite effects of enhanced (weakened) photochemistry above (below) clouds. The global mean photolysis frequencies for  $J[\text{O}^1\text{D}]$  and  $J[\text{NO}_2]$  in the troposphere change by less than 5% because of clouds; global mean  $\text{O}_3$  concentrations in the troposphere increase by less than 5%. This study shows tropical upper tropospheric  $\text{O}_3$  to be less sensitive to the radiative effect of clouds than previously reported ( $\sim 5\%$  versus  $\sim 20\text{--}30\%$ ). These results emphasize that the dominant effect of clouds is to influence the vertical redistribution of the intensity of photochemical activity while global average effects remain modest, again contrasting with previous studies. Differing vertical distributions of clouds may explain part, but not the majority, of these discrepancies between models. Using an approximate random overlap or a maximum-random overlap scheme to take account of the effect of cloud overlap in the vertical reduces the impact of clouds on photochemistry but does not significantly change our results with respect to the modest global average effect.

**Citation:** Liu, H., et al. (2006), Radiative effect of clouds on tropospheric chemistry in a global three-dimensional chemical transport model, *J. Geophys. Res.*, *111*, D20303, doi:10.1029/2005JD006403.

### 1. Introduction

[2] Clouds play critical roles in influencing not only the earth's climate through modulation of the earth's energy

and hydrological cycles but also tropospheric photochemistry through modification of solar radiation that determines photolysis frequencies [e.g., Thompson, 1984; Crawford *et al.*, 1999; Yang and Levy, 2004]. The uncertainty in

<sup>1</sup>National Institute of Aerospace, Hampton, Virginia, USA.

<sup>2</sup>NASA Langley Research Center, Hampton, Virginia, USA.

<sup>3</sup>NASA Goddard Space Flight Center, Greenbelt, Maryland, USA.

<sup>4</sup>Also at Goddard Earth Sciences and Technology Center, University of Maryland, Baltimore County, Maryland, USA.

<sup>5</sup>Department of Earth and Planetary Sciences and Division of Engineering and Applied Sciences, Harvard University, Cambridge, Massachusetts, USA.

<sup>6</sup>Now at School of Earth and the Environment, University of Leeds, Leeds, UK.

<sup>7</sup>Science Applications International Corporation, Hampton, Virginia, USA.

<sup>8</sup>Department of Atmospheric, Oceanic, and Space Sciences, University of Michigan, Ann Arbor, Michigan, USA.

<sup>9</sup>Now at Scripps Institution of Oceanography, University of California, San Diego, La Jolla, California, USA.

<sup>10</sup>National Center for Atmospheric Research, Boulder, Colorado, USA.

radiative processes associated with clouds has been widely recognized as one of the key issues in current assessments of climate change [Cess *et al.*, 1996; Houghton *et al.*, 2001]. The radiative effect of clouds on tropospheric photochemistry and the associated uncertainty have been paid much less attention in the literature. A quantitative understanding of this effect is required for using global models to assess anthropogenic perturbations to the Earth system. We address here this issue with a global three-dimensional (3-D) chemical transport model or CTM (GEOS-CHEM) [Bey *et al.*, 2001a] driven by assimilated meteorological observations.

[3] Clouds affect tropospheric chemistry in a variety of ways. They provide surfaces for heterogeneous chemistry to take place [Jacob, 2000]. Precipitating clouds scavenge soluble trace gases and aerosols from the troposphere [e.g., Liu *et al.*, 2001]. The vertical motions associated with clouds result in substantial convective transport of chemical species. In particular, deep convection can provide an important source of hydrogen oxide radicals in the upper troposphere, leading to enhanced production of ozone [Prather and Jacob, 1997]. Lightning associated with deep convective clouds is an important source of nitrogen oxides in the middle and upper troposphere [e.g., Pickering *et al.*, 1998]. Clouds also scatter and absorb incoming solar radiation, modifying the actinic flux and thus photolysis frequencies of key chemical species. The enhanced photolysis frequencies have been observed above and in the upper levels of clouds, while reduced frequencies were found below optically thick clouds and absorbing aerosols [e.g., Junkermann, 1994; Lefter *et al.*, 2003]. Since photolytical processes are the sources of free radicals, clouds play an important role in determining the oxidative capacity of the troposphere [Thompson *et al.*, 1990].

[4] In order to account for the spatial and temporal variability of photolysis frequencies under different atmospheric conditions, tropospheric chemistry models require photolysis schemes that are computationally efficient. Earlier CTMs often calculated photolysis frequencies offline and then tabulated them for interpolation during model integration for varying solar zenith angles [e.g., Penner *et al.*, 1991; Brasseur *et al.*, 1998]. As Wild *et al.* [2000] pointed out, however, precalculation does not interactively take into account the effects of the simulated ozone column or cloud/aerosol loading, although using more detailed parameterizations or a correction factor during model integration may partly address the problem [Berntsen and Isaksen, 1997; Landgraf and Crutzen, 1998; Feng *et al.*, 2004]. A new scheme for calculating photolysis frequencies online (Fast-J) that is fast, flexible, and deals accurately with multiple scattering, was developed by Wild *et al.* [2000]. Fast-J has been incorporated into a number of CTMs [Wild *et al.*, 2000; Shindell *et al.*, 2001], including the GEOS-CHEM model [Bey *et al.*, 2001a] used in this study. Another efficient photolysis scheme (fast-TUV) using similar methodology and based on the Tropospheric Ultraviolet-Visible Model (TUV) was recently developed by Tie *et al.* [2003].

[5] Several previous modeling studies have examined the radiative effect of clouds on photolysis frequencies and/or oxidants in the troposphere. Tang *et al.* [2003] used a 3-D regional CTM (STEM) coupled with the TUV model to

study the influences of aerosols and clouds on photolysis frequencies and photochemical processes over the Asian-Pacific Rim during the TRACE-P period (February–April 2001). Linear scaling of the cloud optical depth in a grid box with cloud fraction (or uniform cloud distribution; referred to as LIN hereinafter) was assumed. They found that clouds have a large impact on photolysis frequencies with  $J[\text{NO}_2]$  decreased by 20% below clouds and enhanced by  $\sim 30\%$  from 1 km to 8 km. Clouds were also found to reduce OH by 23% at  $<1$  km and increase OH by  $\sim 25\%$  above 1 km. Mao *et al.* [2003] conducted sensitivity experiments of clouds with a radiative transfer model and found that the impact of low and middle clouds on photolysis frequencies was stronger than high clouds by a factor of 2–3 because of large optical depths. Tie *et al.* [2003] suggested that the impact of clouds is probably unrealistically large when LIN is applied to calculate the photolysis frequencies in their global CTM (MOZART-2 coupled with fast-TUV).

[6] One of the important issues or uncertainties when examining the radiative effect of clouds in models concerns how to represent the vertical coherence of clouds. A number of schemes have been introduced to address the effects of vertical subgrid variability of cloudiness on radiative transfer. The most commonly used schemes are the random overlap (RAN) and the maximum-random overlap (MRAN) assumptions [e.g., Geleyn and Hollingsworth, 1979; Briegleb, 1992; Liang and Wang, 1997; Stubenrauch *et al.*, 1997; Collins, 2001; Stephens *et al.*, 2004]. Stephens *et al.* [2004] presented an assessment of these and other different approaches for parameterizing the effects of cloud overlap on radiative transfer in a single radiation model. Photochemical models have just begun to take account of the effect of cloud overlap assumptions [Tie *et al.*, 2003; Feng *et al.*, 2004].

[7] Tie *et al.* [2003] considered the subgrid vertical distribution of clouds by using MRAN in the calculation of photolysis frequencies in a global CTM. They found that with MRAN clouds increase global mean OH concentrations by about 20%, photolysis rates of  $J[\text{O}^1\text{D}]$  and  $J[\text{NO}_2]$  in the troposphere by about 12–13%, and tropospheric  $\text{O}_3$  concentrations by 8%. It was suggested that clouds have important impacts on tropospheric chemistry. They also argued that LIN tends to significantly overestimate back-scattering above clouds and the overall impact on photochemistry in the troposphere. This argument was based on their calculation that showed the estimated global OH with LIN is about 50% higher than that with MRAN. Feng *et al.* [2004] were the first to systematically evaluate the effect of different cloud overlap assumptions (LIN, RAN and MRAN) on averaged photolysis frequencies and OH concentrations in a global photochemical model. Photolysis frequencies are increased in the upper tropical troposphere and decreased in the lower troposphere if LIN or RAN is followed rather than MRAN.

[8] In this study, we apply GEOS-CHEM coupled with Fast-J to quantify the radiative effect of clouds on photolysis rates and key oxidants in the troposphere and to examine the effect of various cloud overlap assumptions. These are essentially the same issues investigated by Tie *et al.* [2003] and Feng *et al.* [2004]. Our results, however, contrast with those of Tie *et al.* [2003] in finding that the dominant effect of clouds is to influence the vertical

redistribution of the intensity of photochemical activity while the global average effect remains modest. In particular, we will show that tropical upper tropospheric ozone concentrations in GEOS-CHEM are much less sensitive to the radiative effect of clouds than those in MOZART-2 as reported by *Tie et al.* [2003]. With online calculation of photolysis frequencies, we also improve over the study of *Feng et al.* [2004] with respect to the impact of different cloud overlap schemes.

[9] The remainder of this paper is organized as follows. Section 2 will briefly describe the GEOS-CHEM model, the Fast-J algorithm, and the cloud overlap assumptions used. Section 3 will present the global distribution of cloud and its evaluation with satellite observations. One-dimensional test cases for offline calculation of photolysis frequencies using Fast-J are examined in section 4. The global impact of GEOS-3 clouds on photolysis frequencies under different cloud overlap assumptions is assessed in section 5. The radiative effect of clouds on tropospheric key oxidants is examined in section 6, followed by discussion in section 7, and summary and conclusions in section 8.

## 2. Model and Methods

### 2.1. GEOS-CHEM

[10] GEOS-CHEM is a global 3-D model of tropospheric  $O_3$ - $NO_x$ -hydrocarbon chemistry coupled to aerosol chemistry. The model is driven by assimilated meteorological observations from the Goddard Earth Observing System (GEOS) of the NASA Global Modeling and Data Assimilation Office (GMAO). This study is based on GEOS-CHEM version 5.5 (see <http://www-as.harvard.edu/chemistry/trop/geos>) driven by 2000 and 2001 GEOS-3 meteorological data.

[11] *Bey et al.* [2001a] presented a first description of the model as applied to simulation of tropospheric  $O_3$ - $NO_x$ -hydrocarbon chemistry. The model was updated by *Martin et al.* [2002], and by *Park et al.* [2004] where aerosol (including sulfate-nitrate-ammonium, carbonaceous aerosols, sea salt, and mineral dust) chemistry is coupled with  $O_3$ - $NO_x$ -hydrocarbon chemistry. The GEOS-3 data, including cloud fields, have 6-hour temporal resolution (3-hour resolution for surface fields and mixing depths),  $1^\circ$  latitude by  $1^\circ$  longitude horizontal resolution, and 48 sigma vertical levels extending up to 0.01 hPa. For computational efficiency, we degrade the horizontal resolution to  $4^\circ \times 5^\circ$  and merge the 26 vertical levels above 85 hPa, retaining a total of 30. The midpoints of the lowest eight levels in the GEOS-3 data are at 10, 50, 100, 200, 350, 600, 850, and 1250 m above the surface for a column based at sea level. All simulations in this study were conducted for August 2000 to December 2001 using standard model output as initial conditions. August–December 2000 was used for initialization and we analyze the model results for the year of 2001.

[12] The model solves the chemical evolution of over 80 chemical species with a fast Gear solver and transports 31 chemical tracers. The model uses the advection scheme of *Lin and Rood* [1996]. The moist convective mixing scheme is that of *Allen et al.* [1996]. Wet deposition of soluble species includes scavenging in wet convective updrafts, and first-order rainout and washout

from both convective and large-scale precipitation [*Liu et al.*, 2001; *Park et al.*, 2004]. The Synoz (synthetic  $O_3$ ) scheme [*McLinden et al.*, 2000] is used as a flux upper boundary condition for  $O_3$  in the stratosphere by imposing a global cross-tropopause flux of 475 Tg  $O_3$  per year. We impose a uniform global  $CH_4$  concentration of 1700 ppbv. Procedures for specifying emissions are described in *Bey et al.* [2001a]. This version of the model also includes an improved biomass burning emission inventory with seasonal variability constrained by satellite observations [*Duncan et al.*, 2003]. Lightning  $NO_x$  source is 6 Tg N  $yr^{-1}$  [*Martin et al.*, 2002].

[13] A global evaluation of the GEOS-CHEM simulation of tropospheric  $O_3$ - $NO_x$ -hydrocarbon chemistry was first presented by *Bey et al.* [2001a]. The model reproduces the climatological monthly mean  $O_3$  concentrations from the ozonesonde observations to within usually 10 ppbv, and captures the phase of the seasonal cycle to within 1–2 months, with the seasonal amplitude underestimated at northern midlatitudes. More specific evaluations of model results (using GEOS-1, GEOS1-STRAT, or GEOS-3) with  $O_3$  observations in different regions of the world have been conducted for the Asian Pacific [*Bey et al.*, 2001b; *Liu et al.*, 2002, 2004], the Middle East [*Li et al.*, 2001], the United States [*Fiore et al.*, 2002a, 2002b, 2003a, 2003b], the North Atlantic [*Li et al.*, 2002a, 2002b], and the tropics [*Martin et al.*, 2002; *Chandra et al.*, 2003]. A detailed description and global evaluation of the model simulation for CO is presented by B. N. Duncan et al. (Model study of the budget, interannual variability, and trends of carbon monoxide, 1988–1997, submitted to *Journal of Geophysical Research*, 2006). The low CO and high OH in the old version of the model [*Bey et al.*, 2001a] has been improved in the current version by the consideration of minor sources from oxidation of previously neglected volatile organic compounds.

### 2.2. Photolysis Calculation

[14] Photolysis frequencies in GEOS-CHEM are calculated with the Fast-J radiative transfer algorithm of *Wild et al.* [2000], which uses a seven-wavelength quadrature scheme and accounts accurately for Rayleigh scattering as well as Mie scattering by aerosols and clouds. Fast-J achieves the accuracy of the calculated photolysis frequencies generally to within 3% [*Wild et al.*, 2000] and compares well with other photolysis schemes [*Olson et al.*, 1997].

[15] A total of 52 photolysis reactions are included in GEOS-CHEM (The GEOS-CHEM Chemical Mechanism version 5-05-03, by Arlene Fiore and Daniel Jacob, Harvard University, June 2003; electronic copy of this document available at [http://www-as.harvard.edu/chemistry/trop/geos/geos\\_mech.html](http://www-as.harvard.edu/chemistry/trop/geos/geos_mech.html)). Photolysis calculations are performed every hour and thus diurnal variations are represented. Vertically resolved cloud optical depths and cloud fractions are taken from the GEOS-3 meteorological archive with 6-hour resolution. Clouds are assumed to be fully scattering. Monthly mean surface albedos are those of *Herman and Celarier* [1997]. This version of GEOS-CHEM uses climatological ozone concentrations as a function of latitude, altitude, and month to calculate the absorption of UV radiation by ozone. We find by sensitivity experiments that using tropospheric ozone concentrations from the model simulation

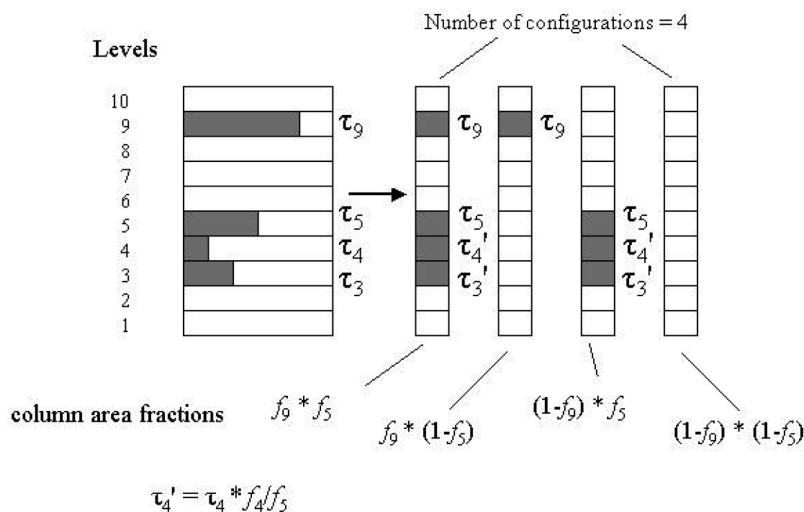


**Figure 1.** Schematic illustration of implementation of the maximum-random cloud overlap scheme (MRAN) as used by *Tie et al.* [2003] for actinic flux calculations [after *Feng et al.*, 2004]. Layers 3, 4, 5 and 9 are cloudy in a ten-layer column. The in-cloud optical depth and cloud fraction at vertical layer  $i$  are indicated by  $\tau_i$  and  $f_i$  ( $i = 1, 2, \dots, 10$ ). This vertical profile of cloudiness is transformed into four configurations. Within the cloud block containing adjacent cloudy layers ( $i = 3, 4$ , and  $5$ ), the cloud fractions are set to the maximum cloud fraction of those layers ( $f_5$ ), and their cloud optical depths (or water contents) are accordingly adjusted. Actinic fluxes for the original column are the averages of those for all four configurations, weighted by the respective column area fractions.

(versus climatology) has little effect on our results presented in this paper.

### 2.3. Cloud Overlap Assumptions

[16] Following *Feng et al.* [2004], we examine in this study three assumptions about the vertical subgrid variability of clouds including the linear scheme, the approximate random overlap scheme, and the maximum-random overlap scheme and evaluate their effects on photolysis frequencies and key oxidants. These schemes are discussed in detail by *Feng et al.* [2004] and *Tie et al.* [2003] and are briefly summarized here as follows.

#### 2.3.1. Linear Assumption (LIN)

[17] The most commonly used assumption in current CTMs is that clouds cover an entire horizontal grid with a cloud optical depth averaged over the clear and cloudy areas in each layer, which assumes that the actinic flux is linearly proportional to cloud optical depth [*Feng et al.*, 2004]. That is, the grid average cloud optical depth  $\tau'_c = \tau_c \cdot f$ , where  $\tau_c$  is the cloud optical depth in the cloudy portion of the grid and  $f$  is the cloud fraction in each layer. This approach may introduce a significant bias because of the nonlinear relationship between photolysis frequencies and cloud optical depth.

#### 2.3.2. Approximate Random Overlap (RAN)

[18] The random overlap scheme assumes that clouds in vertical layers are independent of each other and randomly overlapped. A detailed implementation of this scheme therefore requires extensive computations [*Feng et al.*, 2004]. *Briegleb* [1992] designed a formulation for cloud optical depth, i.e.,  $\tau'_c = \tau_c \cdot f^{3/2}$ . *Briegleb* [1992] showed that this formulation yields a reasonable approximation to a detailed random overlap calculation for the heating rate. As *Feng et al.* [2004] demonstrated, for large cloud fractions, the scaling of cloud optical depth by cloud fraction to

the  $3/2$  power is a good approximation to the exact random overlap calculation; for small cloud fraction, there are large errors. On a global scale cloud fraction is typically 60–70% (see section 3) so that one would expect the approximation is often a good one. This method has been widely used as an approximation for the exact random overlap in global CTMs [e.g., *Brasseur et al.*, 1998], and is also adopted in this study (hereinafter referred to as RAN).

#### 2.3.3. Maximum-Random Overlap (MRAN)

[19] The maximum-random overlap scheme assumes that clouds in adjacent layers are maximally overlapped to form a cloud block and that blocks of clouds separated by clear layers are randomly overlapped [*Geleyn and Hollingsworth*, 1979]. A vertical profile of fractional cloudiness is converted into a series of column configurations with corresponding fractions (Figure 1). Any individual layer has either full or zero cloud cover. Radiative transfer calculation is conducted for each column configuration. Photolysis frequencies are then the average of all column radiation transfer calculations weighted by the column area fraction in each configuration. *Feng et al.* [2004] applied a version of MRAN [*Collins*, 2001] to study the effect of cloud overlap in their photochemical model. *Tie et al.* [2003] used a similar version of MRAN [*Stubenrauch et al.*, 1997] in their study of the radiative effect of clouds on photolysis rates and tropospheric oxidants. The major difference between the two versions of MRAN is that the latter assumes that within a cloud block the cloud fraction is equal to the maximum cloud fraction within those cloud layers and the water content in each cloud layer within the block is adjusted to conserve the total water content. The resulting number of configurations is significantly smaller for the latter than for the former. We find that the different assumptions about the overlap within a cloud block have less than 2–5% effect on monthly, zonal, and daily mean

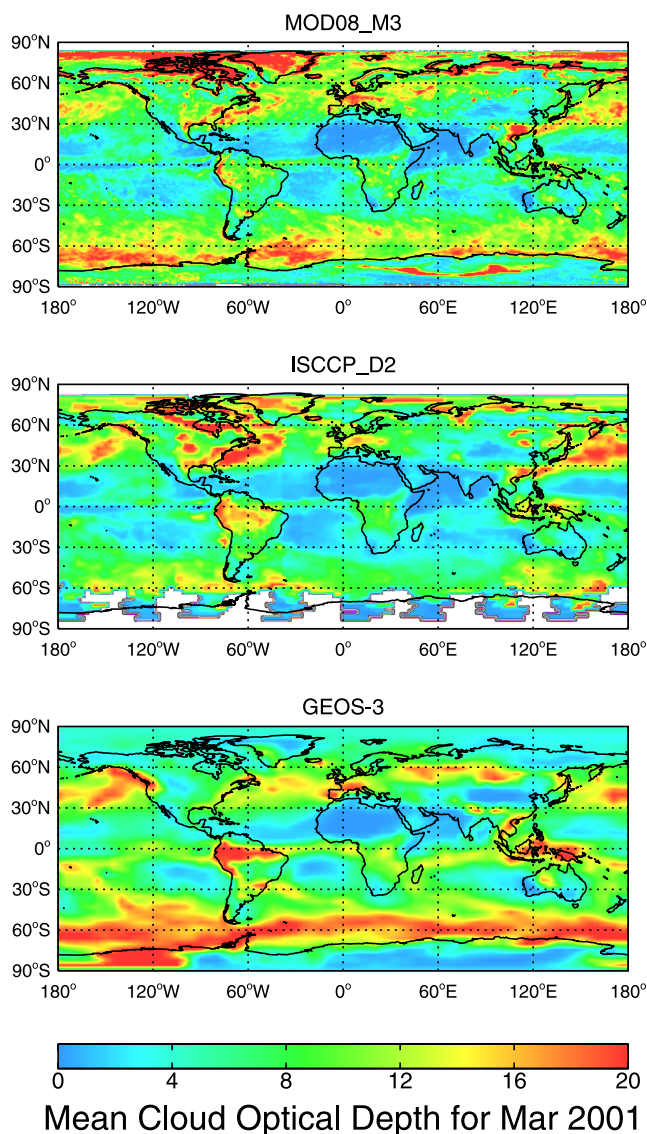


**Figure 2.** (top) MODIS (MOD08\_M3, level-3 monthly global product at  $1^\circ \times 1^\circ$  resolution) and (middle) ISCCP (D2, 280 km equal-area grid) retrievals of cloud optical depth compared to (bottom) GEOS-3 monthly mean grid-scale cloud optical depths for March 2001. ISCCP cloud optical depths shown here are based on linearly averaged values of individual pixels and are about a factor of 2–3 larger than those based on radiative nonlinearly averaged values, which were originally reported by ISCCP. See text for details.

photolysis rates. At a specific location, the vertically integrated photolysis rates can change by up to 8%. If not otherwise explicitly stated, we refer MRAN in the following discussions to the *Stubenrauch et al.* [1997] approach as used by *Tie et al.* [2003] that requires much less computing time.

### 3. Global Cloud Distribution and Evaluation With Satellite Observations

[20] Cloud optical depth and cloud fraction are critical parameters needed to describe the radiative effect of clouds

on tropospheric photochemistry. Fast-J requires as input the grid-scale cloud optical depth in vertical model layers. Model estimates of cloudiness and its vertical variability, however, have large uncertainties. We evaluate in this section the GEOS-3 cloud optical depth and cloud fraction with satellite retrieval products from the Moderate Resolution Imaging Spectroradiometer (MODIS, on Terra) [*Platnick et al.*, 2003] and the International Satellite Cloud Climatology Project (ISCCP) [*Rossow et al.*, 1996; *Rossow and Schiffer*, 1999].

[21] The occurrence of clouds in GEOS-3 is empirically diagnosed on the basis of grid-scale relative humidity and subgrid-scale convection (L. Takacs, personal communication, 2004). The cloud optical properties are empirically prescribed to obtain a reasonable simulation of top-of-the-atmosphere longwave and shortwave cloud forcing. For large-scale clouds, cloud optical depth is empirically assigned values proportional to the diagnosed large-scale liquid water. For convective clouds, cloud optical depth is prescribed as 16 per 100 mbar. A temperature dependence is used to distinguish between water and ice clouds.

[22] We show in Figure 2 the global distribution of GEOS-3 monthly mean (grid-scale) cloud optical depths as compared to MODIS (MOD08\_M3, level-3 monthly global product at  $1^\circ \times 1^\circ$  resolution) and ISCCP (D2, 280 km equal-area grid) retrievals for March 2001 when frequent cyclogenesis occurred in the Northern Hemisphere (NH). Zonal mean plots for March, June, October, and December of 2001 are shown in Figure 3. The MODIS and ISCCP values are the scalar product of the cloud optical depth retrievals and their respective cloud fractions; thus they represent average conditions accounting for both cloudy and clear conditions. This is necessary for a consistent comparison with model monthly mean optical depths. Using ISCCP 3-hourly monthly

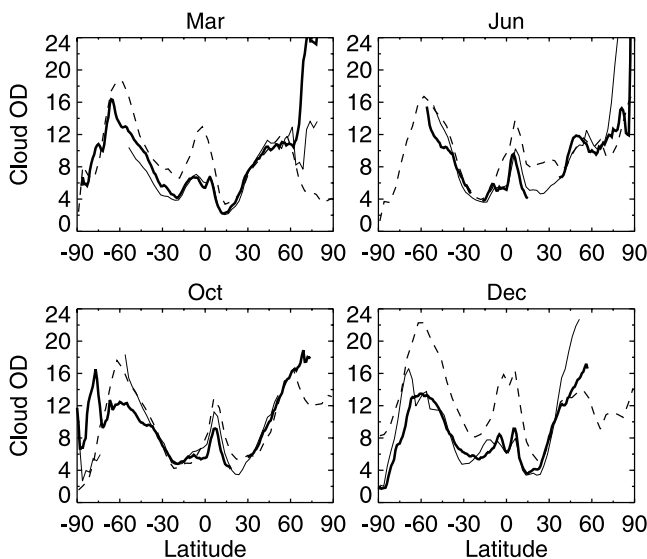


**Figure 3.** Same as Figure 2 but shown as zonal mean plots for March, June, October, and December of 2001. MODIS, ISCCP, and GEOS-3 cloud optical depths are thick, thin, and dashed lines, respectively. ISCCP values for October and December are from the year 2000. See text for details.

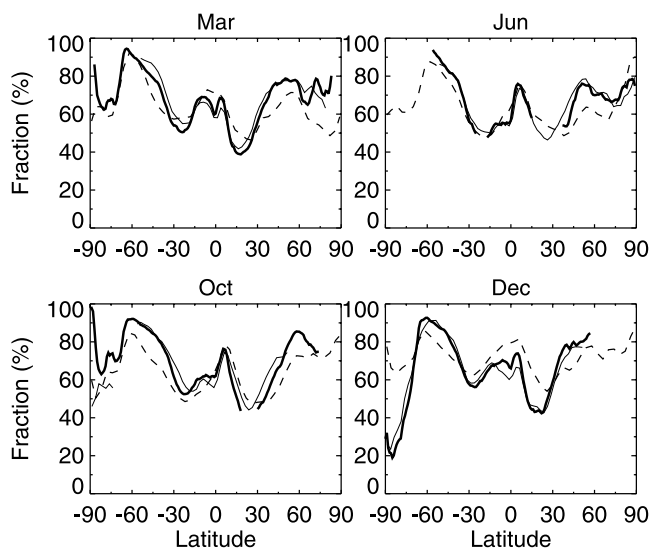


**Figure 4.** Same as Figure 3 but for monthly mean cloud fraction. MODIS, ISCCP, and GEOS-3 cloud fractions are thick, thin, and dashed lines, respectively. ISCCP values for October and December are from the year 2000.

mean cloud retrievals sampled at the Terra MODIS local equatorial crossing time (approximately 10:30am) has little effect on our results reported here. Both MODIS and ISCCP cloud optical depths reveal the maxima associated with tropical convection, extratropical cyclones in NH, and the marine stratiform clouds in the Southern Hemisphere (SH,  $\sim 50\text{--}60^\circ\text{S}$ ). GEOS-3 shows the same features in cloud optical depths but tends to overestimate the values at  $\sim 50\text{--}60^\circ\text{S}$  as well as in the tropics. At northern high latitudes, GEOS-3 cloud optical depths do not show values as high as those from MODIS and ISCCP retrievals; the latter is presumably due to uncertainties associated with snow or ice cover in the satellite retrievals for these regions. GEOS-3 appears to capture the day-to-day variability in cloud optical depth associated with synoptic-scale frontally induced cloudiness in the Asian Pacific region during spring (not shown). Similar plots are constructed for monthly mean cloud fraction. GEOS-3 cloud fraction agrees, overall, with MODIS and ISCCP products, but tends to be somewhat lower at midlatitudes (Figure 4).

[23] While the MODIS and ISCCP monthly mean cloud optical depths presented in Figures 2 and 3 are comparable in magnitude, note that it was first necessary to make some adjustments to the cloud optical depths reported by these two projects in order to make them directly comparable. This is because ISCCP values are based on radiative non-linearly averaged values of individual pixels while the MODIS values used were based on linear averages. This difference in averaging has led to previous reports of large differences (a factor of 2–3) between MODIS and ISCCP monthly mean cloud optical depths [Pinker *et al.*, 2003]. While the cloud optical depths reported in the ISCCP D2 data set are averaged values of individual pixels with nonlinear weights that preserve the average cloud albedo, linear averages of individual pixel values of optical depth proportional to cloud water content are stored in the ISCCP

D2 data set as water path [Rossow *et al.*, 1996]. Thus to be consistent with the linearly averaged MODIS optical depths, we have used linearly averaged cloud optical depth derived from the ISCCP water path data.

[24] The above evaluations of GEOS-3 cloud optical depth and cloud fraction provide a quantitative estimate of errors in these fields, which are used in the radiative transfer calculations. One caveat, however, is that the range of visible optical depths that can be measured by satellites is typically  $\sim 0.5\text{--}100$ , limited by cloud detection limits at the lower end and lack of further sensitivity at the upper end [Hartmann *et al.*, 1999]. On the other hand, there is at present a lack of information about the global climatology of the vertical distribution of cloud amount and optical depth, preventing a reliable evaluation of cloud vertical distributions in GEOS-3.

## 4. Effect of Cloud on Photolysis Rates: Test Cases

### 4.1. Effect of Cloud Overlap

[25] We use the one-dimensional test cases designed by Feng *et al.* [2004] to evaluate Fast-J photolysis frequencies calculation and the effect of different cloud overlap assumptions. As Feng *et al.* [2004] showed, the effect of cloud overlap is sensitive to cloud fraction as well as to solar zenith angle. We illustrate this for  $J[\text{O}^1\text{D}]$  in Figures 5 and 6 for  $0^\circ$  and  $60^\circ$  solar zenith angles, respectively. Atmospheric conditions are based on those of  $45^\circ\text{N}$  summer. Total ozone column is 330 DU. Surface albedo is 0.1. We assume here clouds are fully scattering and do not include aerosols. In Figures 5a, 5b, 6a, and 6b, clouds with a large mean optical depth of 54 are placed between 2–3 km and 3–4 km with either small cloud fraction (0.1 and 0.2, respectively) or large cloud fraction (0.8 and 0.9, respectively). In Figure 5c and 6c, clouds with a small mean optical depth of 6 are placed between 2–3 km and 3–4 km with cloud fractions of 0.2 and 0.3, respectively.

[26] Relative to clear-sky conditions, the presence of the optically thick cloud leads to enhancement of  $J[\text{O}^1\text{D}]$  above the cloud (as well as in the upper part of the cloud) and reduction below the cloud. In the case of small cloud fraction, this effect of clouds on  $J[\text{O}^1\text{D}]$  is substantially larger in LIN and RAN than in MRAN because clouds extend to the entire layer in the former two schemes, leading to more reflection of solar radiation from the cloud below and less radiation penetrating through the cloud (Figure 5a). RAN gives  $J[\text{O}^1\text{D}]$  that are closer to those in MRAN because of the scaling of cloud optical depth by cloud fraction to the  $3/2$  power in RAN. In the case of large cloud fraction, the differences in both the enhancement of  $J[\text{O}^1\text{D}]$  above the cloud and the reduction below the cloud are relatively small (Figure 5b). Because global cloud coverage is about 60–70%, this may have an important implication for the global effects of cloud overlap treatment. In case of small cloud optical depth (Figure 5c), the cloud column optical depth is larger in MRAN than in RAN because of line-up of clouds in adjacent layers [Feng *et al.*, 2004]. MRAN therefore gives larger enhancements (reductions) of  $J[\text{O}^1\text{D}]$  than RAN does above (below) the cloud. LIN continues to give the largest enhancement above the cloud. At the large solar zenith angles of  $60^\circ$  (Figure 6), the reduction of  $J[\text{O}^1\text{D}]$  below the cloud in RAN and LIN is

Effect of cloud overlap on  $J[O^1D]$  calculated by off-line Fast-J

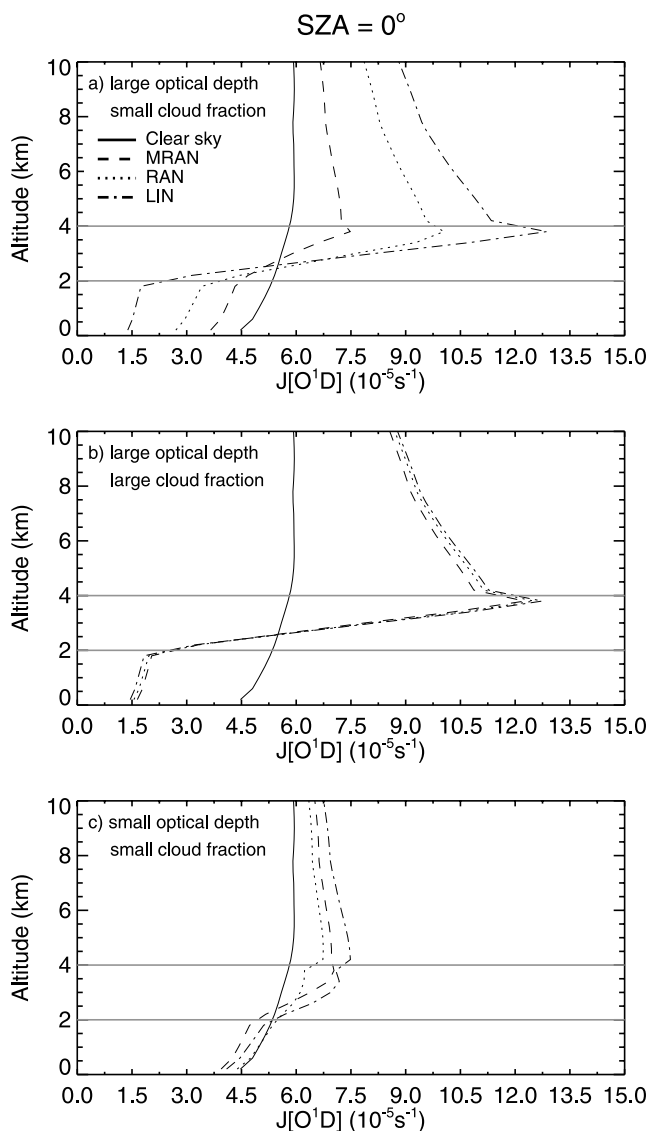


**Figure 5.** Vertical profiles of  $J[O^1D]$  at zero solar zenith angles under clear-sky and cloudy conditions calculated by off-line Fast-J for the test cases of *Feng et al.* [2004]. Cloud overlap assumptions are MRAN (maximum-random), RAN (approximate random), and LIN (linear assumption). Clouds are placed between 2–3 km and 3–4 km (indicated with shaded lines): (a) Cloud fractions are 0.1 (2–3 km) and 0.2 (3–4 km) and column mean optical depth is 54; (b) cloud fractions are 0.8 (2–3 km) and 0.9 (3–4 km) and column mean optical depth is 51; and (c) cloud fractions are 0.2 (2–3 km) and 0.3 (3–4 km) and column mean optical depth is 6.

enhanced compared to MRAN, in particular for small cloud fraction. With small cloud fraction, MRAN gives the largest  $J[O^1D]$  below the cloud (Figure 6c), contrasting with the smallest values at zero solar zenith angle (Figure 5c).

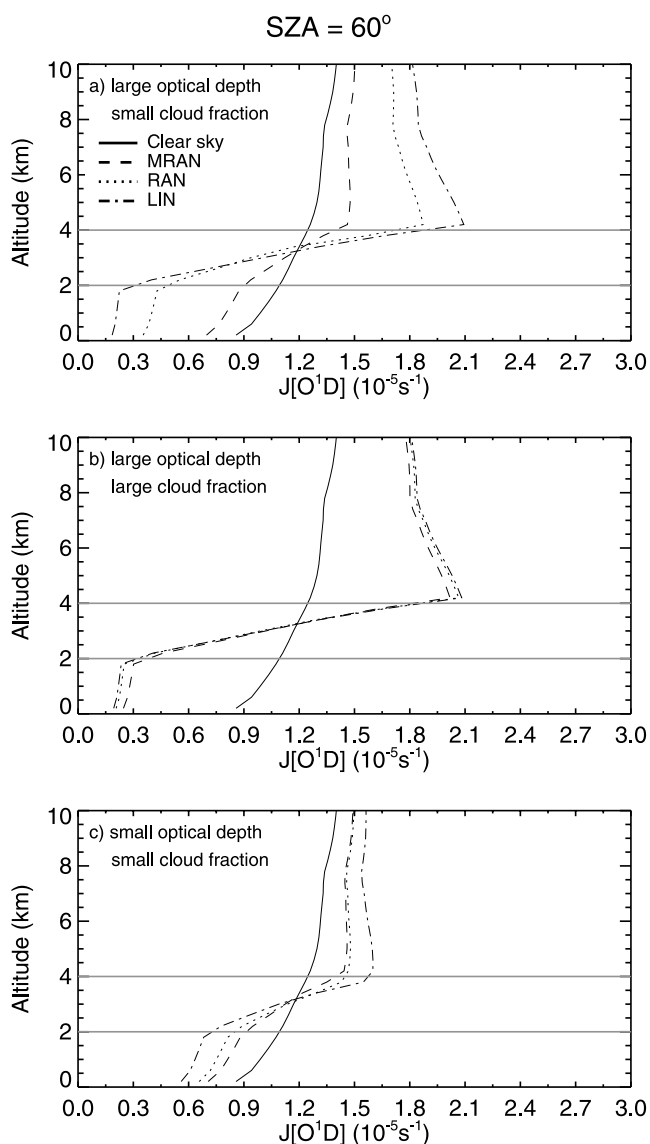
[27] To summarize, our calculation of  $J[O^1D]$  for clear sky and different overlap assumptions using the Fast-J algorithm generally reproduces the features revealed by

the calculation of *Feng et al.* [2004] using the TUV model, lending confidence to the implementation of cloud overlap assumptions in this study. Relative to LIN and RAN, MRAN decreases the radiative impact of clouds on photolysis frequencies for optically thick clouds, but increases the impact below optically thin clouds at small solar zenith angles.

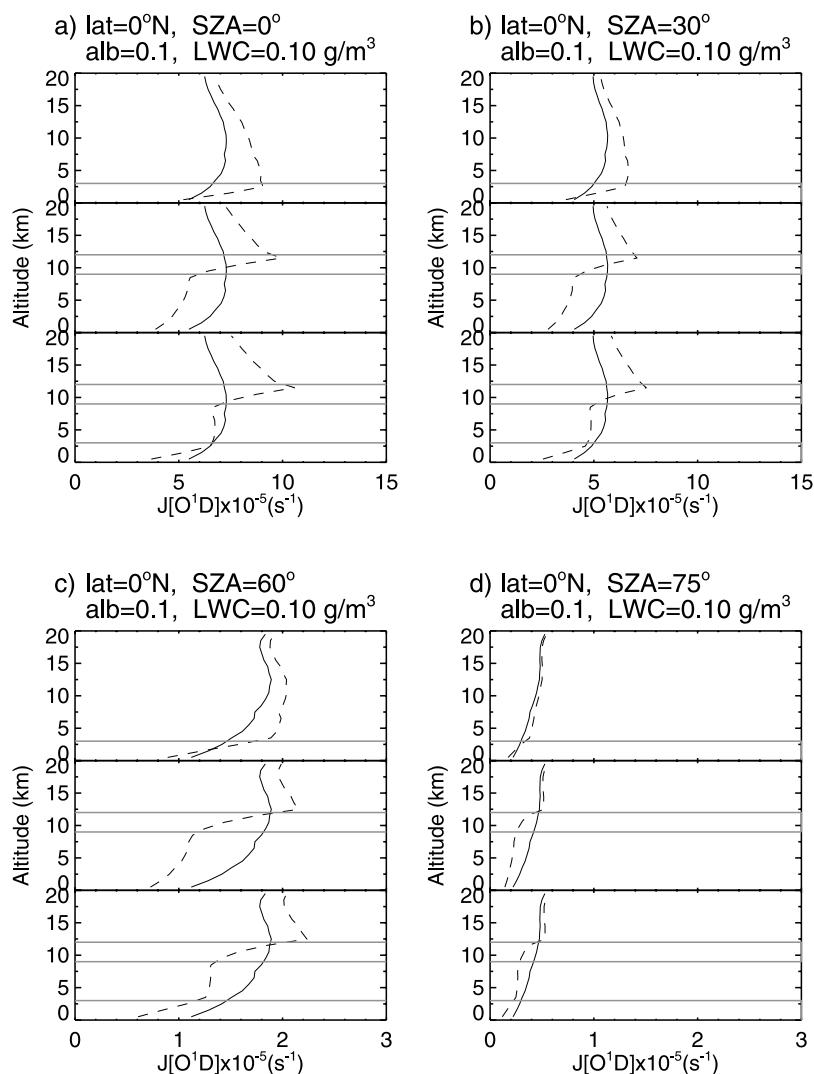
#### 4.2. Sensitivity to Vertical Cloud Distributions and Cloud Water Contents

[28] We assess the sensitivity of the impact of clouds on photolysis rates to different vertical cloud distributions and cloud water contents (or optical depths) by using the test cases designed by *Tie et al.* [2003, 2006]. Three different vertical cloud distributions are assumed: (1) a single cloud layer between 0 and 3 km (low cloud case), (2) a single cloud layer between 9 and 12 km (high cloud case), and

Effect of cloud overlap on  $J[O^1D]$  calculated by off-line Fast-J



**Figure 6.** (a–c) Same as Figure 5 but at a solar zenith angle of 60°.

Effect of clouds on  $J[O^1D]$  calculated by the off-line Fast-J model

**Figure 7.** Vertical profiles of  $J[O^1D]$  at solar zenith angles of (a)  $0^\circ$ , (b)  $30^\circ$ , (c)  $60^\circ$ , and (d)  $75^\circ$  under clear-sky (solid lines) and cloudy (dashed lines, with maximum-random cloud overlap assumption) conditions calculated by off-line Fast-J for the test cases of *Tie et al.* [2003]. Clouds (indicated with shaded lines) are placed between 0–3 km (single low cloud layer), 9–12 km (single high cloud layer), 0–3 km and 9–12 km (multilayer clouds), respectively. Cloud liquid water content is  $0.1 \text{ g/m}^3$ , cloud fraction is 50%, and the effective radius of cloud liquid water droplet is  $20 \mu\text{m}$ , following *Tie et al.* [2003, 2006]. See text for more details.

(3) multilayer clouds between 0–3 km and 9–12 km (multilayer cloud case). Atmospheric conditions are based on those of tropical regions ( $0^\circ\text{N}$ ). The cloud liquid water content is  $0.1 \text{ g/m}^3$ . The cloud optical depth is then obtained by [*Slingo and Schrecker*, 1982]:

$$\tau = \beta dz, \quad \beta = 3 \text{LWC}/(2 r_e),$$

where  $\tau$  is the cloud optical depth,  $\beta$  is the extinction coefficient ( $\text{m}^{-1}$ ), LWC is the cloud liquid water content ( $\text{g/m}^3$ ),  $dz$  is the thickness of cloudy layer (m), and  $r_e$  is the effective radius for cloud liquid water droplets (typically  $\sim 10 \mu\text{m}$ ). Following *Tie et al.* [2003, 2006],

we use in these test cases the MRAN cloud overlap scheme, a cloud fraction of 50%,  $r_e$  of  $20 \mu\text{m}$ , a cloud single scattering albedo (SSA) of 0.999, a surface albedo of 0.1, and a total ozone column of 300 DU. Figure 7 shows the Fast-J calculated  $J[O^1D]$  under both clear and cloudy conditions for three different vertical cloud distributions and at four solar zenith angles ( $0^\circ$ ,  $30^\circ$ ,  $60^\circ$ , and  $75^\circ$ ). Table 1 shows the sensitivity of  $J[O^1D]$  (and  $J[\text{NO}_2]$ ) to the cloud optical depth by changing cloud liquid water content by  $\pm 50\%$ .

[29] With overhead sun, in the case of low cloud layer,  $J[O^1D]$  is enhanced above and throughout much of the cloud, with a maximum near the top of the cloud

**Table 1.** Percentage Changes in  $J[\text{O}^1\text{D}]$  and  $J[\text{NO}_2]$  Due to Clouds Calculated With the Off-Line Fast-J Model and Maximum-Random Overlap (MRAN) Scheme, as a Function of Cloud Vertical Distribution, Cloud Liquid Water Content (LWC), and Solar Zenith Angle (SZA)<sup>a</sup>

SZA	Cloud Vertical Distribution	LWC, $\text{g/m}^3$		
		0.05	0.10	0.15
0°	low cloud <sup>b</sup>	12.6 <sup>c</sup> (21.4 <sup>d</sup> )	18.0 (30.2)	20.4 (34.2)
0°	high cloud <sup>b</sup>	-0.3 (4.5)	-6.1 (-1.1)	-9.9 (-4.9)
0°	multilayer cloud <sup>b</sup>	10.6 (24.5)	7.7 (24.4)	4.6 (21.8)
30°	low cloud	11.2 (18.7)	15.4 (25.4)	17.3 (28.5)
30°	high cloud	-5.0 (-1.6)	-10.5 (-6.9)	-13.9 (-10.2)
30°	multilayer cloud	4.6 (15.5)	1.5 (14.5)	-1.5 (12.0)
60°	low cloud	7.4 (12.6)	9.7 (15.5)	10.8 (16.8)
60°	high cloud	-15.4 (-15.5)	-19.5 (-19.0)	-21.8 (-20.8)
60°	multilayer cloud	-9.0 (-5.2)	-11.6 (-6.8)	-13.6 (-8.3)
75°	low cloud	5.2 (6.2)	7.1 (7.8)	8.0 (8.6)
75°	high cloud	-19.6 (-21.9)	-22.6 (-23.8)	-24.3 (-24.8)
75°	multilayer cloud	-14.7 (-16.5)	-16.5 (-17.3)	-17.9 (-18.2)

<sup>a</sup>Atmospheric conditions are based on those of tropical regions (0°N). Surface albedo is 0.1. Total ozone column is 300 DU. Cloud fraction is 50%. See text for details.

<sup>b</sup>Three different vertical distributions of clouds [after *Tie et al.*, 2003, 2006]. Low cloud case: a single cloud layer between 0 and 3 km; high cloud case: a single cloud layer between 9 and 12 km; and multilayer cloud case: two cloud layers between 0–3 km and 9–12 km.

<sup>c</sup>Percentage changes of 0–16 km averages for  $J[\text{O}^1\text{D}]$ .

<sup>d</sup>Percentage changes of 0–16 km averages for  $J[\text{NO}_2]$ .

(Figure 7a). The total enhancement averaged over the whole troposphere is about 18% (Table 1). For the high cloud case,  $J[\text{O}^1\text{D}]$  increases above the cloud and throughout much of the cloud, and decreases below the cloud. On average,  $J[\text{O}^1\text{D}]$  decreases about 6% in the troposphere. For the multilayer cloud case, a larger  $J[\text{O}^1\text{D}]$  enhancement is seen above the high cloud layer because of radiation reflected from the low cloud layer; the latter also explains the smaller reductions between the two cloud layers.  $J[\text{O}^1\text{D}]$  decreases near the surface. Overall change in  $J[\text{O}^1\text{D}]$  is about 7.7% in the troposphere. The percentage changes in  $J[\text{O}^1\text{D}]$  for these three test cases are comparable to those reported by *Tie et al.* [2003, 2006] with the fast-TUV model (12.7%, -5.7%, and 3.9%, respectively).

[30] As *Tie et al.* [2003] found, the impact of clouds on photolysis is very sensitive to the vertical location of clouds as well as the cloud water content (Table 1). Interestingly, this impact is more sensitive to the vertical location of clouds than to the cloud water content. An important implication, as mentioned earlier, is that having a reasonable vertical distribution of cloudiness is essential for taking account of the radiative effect of clouds. On the other hand, we can see from Table 1 that with increasing solar zenith angles, the enhancement above the low cloud decreases and the reduction below the high cloud increases, because of larger path lengths.

## 5. Global Impact of Clouds on Photolysis Frequencies

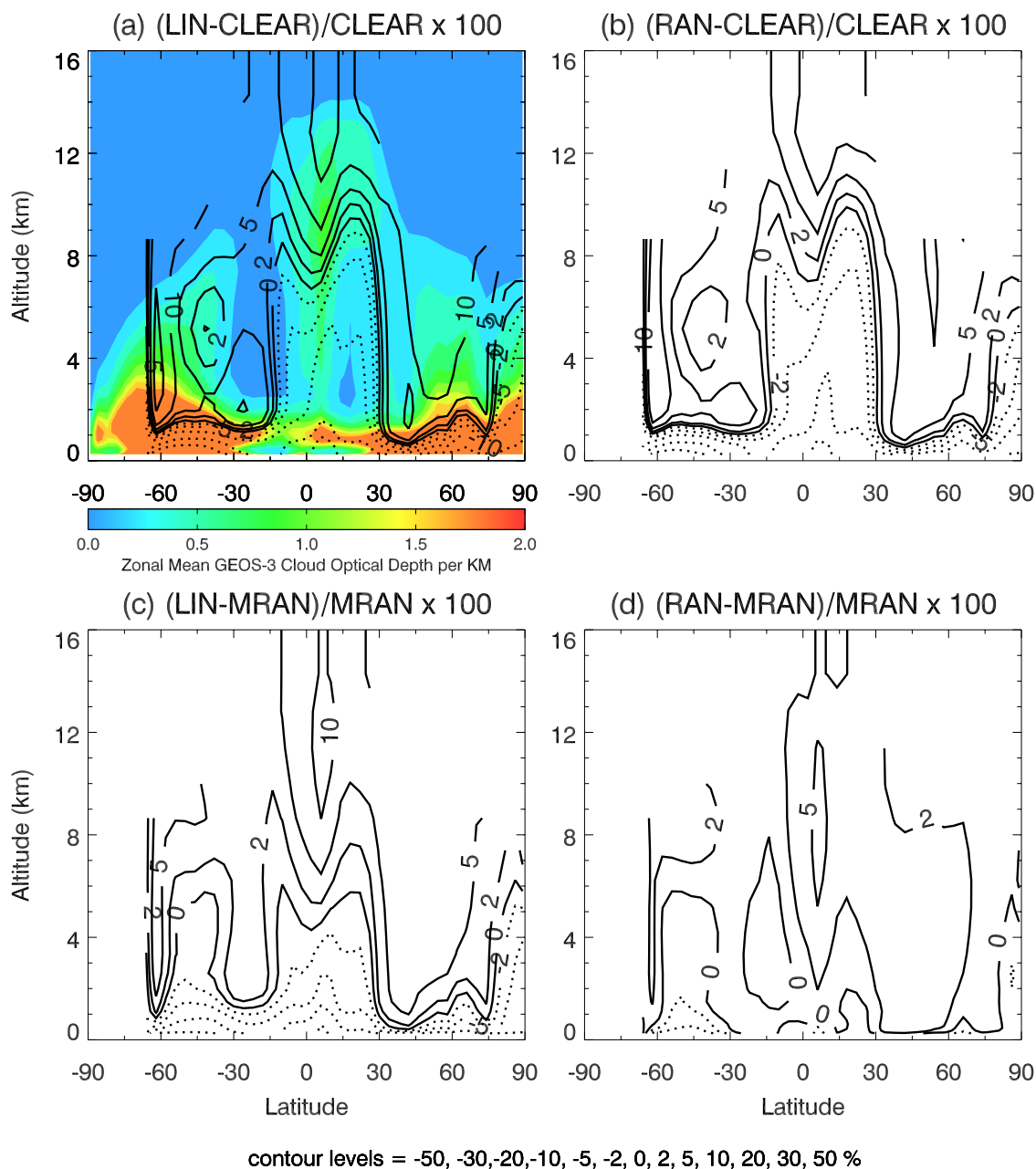
[31] In this section, we assess the global impact of clouds on photolysis frequencies by coupling Fast-J with GEOS-CHEM, including the effect of cloud overlap. We focus on photolysis frequencies  $J[\text{O}^1\text{D}]$  and  $J[\text{NO}_2]$  which are most important for determining OH and O<sub>3</sub> concentrations.

[32] Figures 8a and 8b show the percentage changes in monthly daily mean  $J[\text{O}^1\text{D}]$  due to the radiative effect of

clouds as simulated by GEOS-CHEM with LIN (Figure 8a) and RAN (Figure 8b) for June 2001. Also shown in Figure 8a is the latitude-altitude cross section of zonal mean GEOS-3 cloud optical depth per kilometer. In the tropics,  $J[\text{O}^1\text{D}]$  is enhanced by up to ~20% above the clouds, and reduced by up to ~10–20% below; it reflects the backscattering (attenuation) of solar radiation above (below) the deep convective clouds. Similar effects are also seen above and below the low-level clouds at NH and SH midlatitudes. Above the clouds, NH sees larger enhancements (~10%) than SH does (~5%) in spite of smaller column cloud optical depth in the model (Figure 3); this is because of smaller solar zenith angles in NH at this time of the year (see Table 1). Near the surface,  $J[\text{O}^1\text{D}]$  are reduced by ~20–30% at all latitudes. As expected, using RAN leads to a smaller impact of clouds on  $J[\text{O}^1\text{D}]$  because more solar radiation is able to penetrate through the clouds (Figures 8a and 8b). Nevertheless, LIN and RAN give similar patterns in terms of the regions of  $J[\text{O}^1\text{D}]$  enhancements and reductions due to the radiative impact of clouds.

[33] As *Feng et al.* [2004] pointed out, observational studies have not been able to distinguish whether RAN or MRAN is preferred. We choose to use MRAN as the reference because previous studies found that cloud overlap might best be modeled as a combination of random and maximum overlap [*Hogan and Illingworth*, 2000]. Figures 8c and 8d show the percentage differences in daily mean  $J[\text{O}^1\text{D}]$  between LIN and MRAN, RAN and MRAN, respectively, as simulated by GEOS-CHEM. LIN overestimates reflection of solar radiation above the clouds in particular in the tropics (up to 10%) and overestimates the reduction near the surface by ~10% (Figure 8c). The differences between RAN and MRAN are generally ~2% and not more than ~5% anywhere (Figure 8d). The relatively larger differences (~5%) in the tropical middle and upper troposphere reflect an overestimate of actinic fluxes in RAN relative to MRAN, within deep convective clouds (Figure 8d) which typically have large optical depth and small cloud fraction (see

### J[O<sup>1</sup>D] changes (%), June 2001



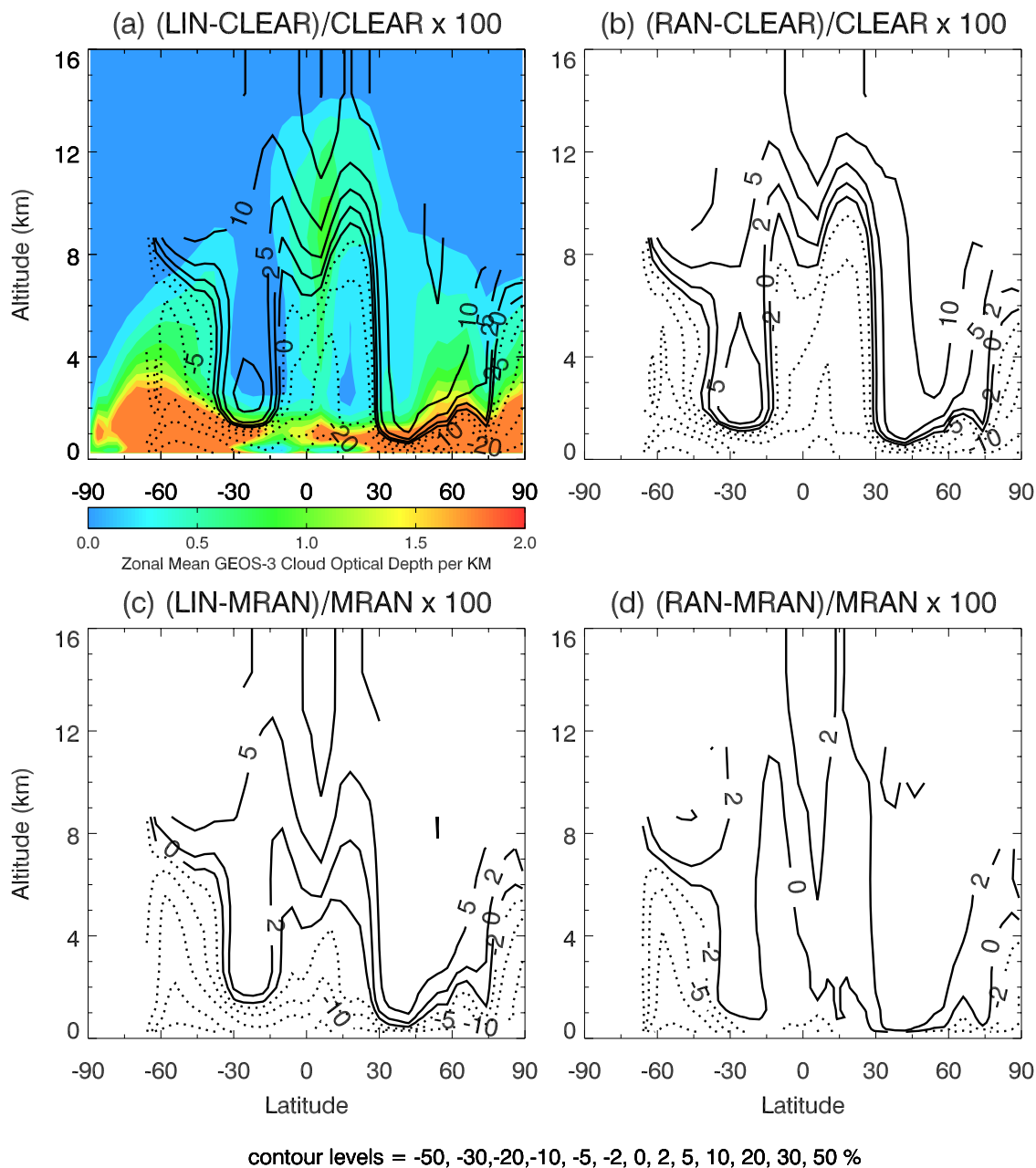
**Figure 8.** Simulated percentage changes in monthly zonal mean  $J[\text{O}^1\text{D}]$  for June 2001 (a) due to the radiative effect of clouds with the linear assumption (LIN), (b) due to the radiative effect of clouds with the approximate random overlap (RAN), (c) between LIN and the maximum-random overlap (MRAN), and (d) between RAN and MRAN. The image in Figure 8a shows the zonal mean GEOS-3 cloud optical depth per kilometer.

Figure 5). Nevertheless, the computationally cheap RAN is overall a good approximation to the more expensive MRAN in terms of the calculated daily mean photolysis rates.

[34] Similar plots are shown in Figure 9 for  $J[\text{NO}_2]$ . The impact of clouds on  $J[\text{NO}_2]$  is comparable to or larger than that on  $J[\text{O}^1\text{D}]$  (Figures 9a and 9b). The major absorption by  $\text{NO}_2$  occurs at longer wavelengths (near 380 nm) than does the absorption by  $\text{O}_3$ ; the former is less dependent on

Rayleigh scattering [Jacob *et al.*, 1989; Feng *et al.*, 2004]. As a result,  $J[\text{NO}_2]$  is more sensitive to the presence of clouds than  $J[\text{O}^1\text{D}]$ , as we can see from Figures 8a and 9a. At southern polar regions where solar zenith angles are large,  $J[\text{NO}_2]$  and  $J[\text{O}^1\text{D}]$  change in opposite directions because of the much larger sensitivity of  $J[\text{NO}_2]$  to the presence of optically thin high clouds than that of  $J[\text{O}^1\text{D}]$ . This may also partly reflect the low accuracy of Fast-J at large solar zenith angles, an aspect that is improved in the

## J[NO<sub>2</sub>] changes (%), June 2001



**Figure 9.** (a–d) Same as Figure 8 but for J[NO<sub>2</sub>].

updated Fast-J algorithm, the so-called Fast-JX. Compared to MRAN, LIN overestimates J[NO<sub>2</sub>] above the clouds (up to ~10% in the tropics) and underestimates J[NO<sub>2</sub>] below the clouds (up to ~10–20% near the surface) (Figure 9c). J[NO<sub>2</sub>] differences between RAN and MRAN are less than ~2% except at southern polar regions with large solar zenith angles (Figure 9d).

### 6. Radiative Effect of Clouds on Key Oxidants

[35] Cloud perturbations to photolysis frequencies affect tropospheric chemistry and, in particular key oxidants in the troposphere. We examine in this section the radiative effect

of clouds on global OH and tropospheric O<sub>3</sub> budget, including the effect of cloud overlap. The radiative effect of clouds is represented by subtraction of the clear-sky simulation from the cloudy-sky simulation.

#### 6.1. Global Mean Effect

[36] Shown in Table 2 are the percentage changes in the global tropospheric mean concentrations of key oxidants and global mean photolysis frequencies due to the radiative effect of clouds in June and December 2001, following Table 4 of *Tie et al.* [2003]. Our calculated global mean changes in OH, O<sub>3</sub>, NO<sub>x</sub>, HO<sub>2</sub>, CH<sub>2</sub>O, and CO are generally less than 6%, independent of the cloud overlap schemes

**Table 2.** Simulated Percentage Changes in the Global Mean Concentrations of Tropospheric Chemical Species, Photolysis Frequencies and Global Mean Lifetimes of Methylchloroform (MCF) and CH<sub>4</sub> Due to the Radiative Effect of Clouds With Different Cloud Overlap Assumptions (LIN, RAN, and MRAN) in June and December 2001, Following Table 4 of *Tie et al.* [2003, 2006]<sup>a</sup>

Quantity	GEOS-CHEM <sup>b</sup> (This Work)			MOZART-2 <sup>c</sup> [ <i>Tie et al.</i> , 2003, 2006]	
	LIN	RAN	MRAN	LIN	MRAN
<i>June</i>					
OH	0.99	0.13	-0.52	88.09	20.31
O <sub>3</sub> <sup>d</sup>	4.8	3.15	3.65	12.07	8.55
NO <sub>x</sub> <sup>e</sup>	5.58	3.46	3.26	-4.17	-3.13
HO <sub>2</sub>	-2.27	-1.60	-1.47	16.52	5.89
CH <sub>2</sub> O	5.55	3.85	4.77	-14.56	-5.78
CO	0.81	1.33	2.26	-31.40	-9.01
J[O <sup>1</sup> D]	3.23	1.72	0.87	44.98	13.38
J[NO <sub>2</sub> ]	5.80	3.04	3.01	62.24	13.84
J[CH <sub>2</sub> O]	5.10	2.65	2.67	54.56	13.75
<i>December</i>					
OH	11.53	7.21	6.93	80.18	20.57
O <sub>3</sub> <sup>d</sup>	3.48	2.05	2.79	12.14	8.53
NO <sub>x</sub> <sup>e</sup>	6.72	4.56	3.77	-12.10	-5.60
HO <sub>2</sub>	1.89	1.27	1.42	12.11	5.09
CH <sub>2</sub> O	3.15	1.81	2.32	-11.90	-4.59
CO	-0.81	-0.15	0.34	-32.43	-10.19
J[O <sup>1</sup> D]	12.49	7.99	7.84	42.76	12.04
J[NO <sub>2</sub> ]	16.24	10.55	10.52	58.99	13.19
J[CH <sub>2</sub> O]	14.84	9.46	9.88	51.48	12.40
MCF lifetime <sup>f</sup>	4.97	3.35	4.23	N/A	N/A
CH <sub>4</sub> lifetime <sup>f</sup>	5.38	3.61	4.49	-45 <sup>g</sup>	-18 <sup>g</sup>

<sup>a</sup>The radiative effect of clouds is represented by subtraction of the clear-sky simulation from the cloudy-sky simulation.

<sup>b</sup>We calculate global mean concentrations by dividing the global total moles of a species by those of air. Global mean photolysis frequencies are volume-weighted values.

<sup>c</sup>Percentage changes reported in *Tie et al.* [2003] were based on the volume mixing ratios averaged over each grid box below 200 mbar (X. Tie, personal communication, 2004). See text for details.

<sup>d</sup>Actually the extended odd oxygen family defined as  $O_x = O_3 + NO_2 + 2 \times NO_3 + \text{peroxyacynitrates} + HNO_4 + 3 \times N_2O_5 + HNO_3$ .

<sup>e</sup>NO<sub>x</sub> = NO + NO<sub>2</sub>.

<sup>f</sup>Percentage changes in global annual mean lifetimes of MCF and CH<sub>4</sub>. The lifetimes are derived as the ratio of the total burden of atmospheric MCF or CH<sub>4</sub> to the tropospheric loss rate against oxidation by OH. Under clear-sky conditions, MCF (CH<sub>4</sub>) lifetimes are 6.5 (11) years in GEOS-CHEM, and CH<sub>4</sub> lifetime is about 11.4 years in MOZART-2 [*Tie et al.*, 2003].

<sup>g</sup>Percentage changes averaged over June and December.

used. The significantly larger changes in OH during December is mainly due to large cloud optical depths associated with the SH marine stratus in GEOS-3. This effect is probably an overestimate because GEOS-3 significantly overestimates these cloud optical depths (Figure 3). For other months, GEOS-3 gives cloud optical depths that are much closer to satellite retrievals (Figure 3). As we will show below, the fact that global mean effect remains modest in our model reflects an offsetting effect of above-cloud enhancements and below-cloud reductions. The same can be said for our calculated global changes in photolysis frequencies (section 5). The lifetime of methylchloroform (CH<sub>3</sub>CCl<sub>3</sub>, MCF) or CH<sub>4</sub> is a proxy for the global mean OH concentrations [*Spivakovsky et al.*, 1990]. We calculate the MCF lifetime as the ratio of the total burden of atmospheric MCF to the tropospheric loss rate against oxidation by OH [*Spivakovsky et al.*, 2000]. Annual mean lifetime of MCF (CH<sub>4</sub>) for 2001 is 6.5 (11) years under clear-sky condition and changes by less than 6% under cloudy-sky condition using any of the cloud overlap schemes (Table 2). Interestingly, we find that the MCF (CH<sub>4</sub>) lifetime may increase even if global mean OH concentrations increase. This reflects the fact that the MCF (CH<sub>4</sub>) lifetime is more sensitive to the OH concentrations in the lower troposphere (versus the middle and upper troposphere) because of the

temperature dependency of the MCF-OH (CH<sub>4</sub>-OH) reaction constant. Our global MCF lifetime is within the range of previous estimates from observations (5–7 years) [*Spivakovsky et al.*, 2000; *Prinn et al.*, 2001].

## 6.2. Zonal Mean Effect

[37] Figures 10a and 10b show the percentage changes in monthly daily mean OH due to the radiative effect of clouds as simulated by GEOS-CHEM with LIN (Figure 10a) and RAN (Figure 10b) for June 2001. In the tropics, OH is enhanced by up to ~5–10% above the deep convective clouds, and reduced by ~5–20% below, reflecting the backscattering (attenuation) of solar radiation above (below) the tropical convective clouds (Figure 10a). At NH midlatitudes, OH is enhanced by ~5–10% above the low-level clouds; at SH subtropics, OH are enhanced by ~5%; at SH high latitudes, the impact of clouds on OH does not show consistent patterns. Near the surface, OH decreases by approximately -20% because of clouds. Using RAN rather than LIN reduces the impact of clouds on OH (Figures 10a and 10b). Compared to MRAN, LIN underestimates OH by up to ~10% near the surface and overestimates OH by 5–10% above the low-level clouds at NH midlatitudes and above the tropical clouds (Figure 10c). RAN gives OH

## OH changes (%), June 2001

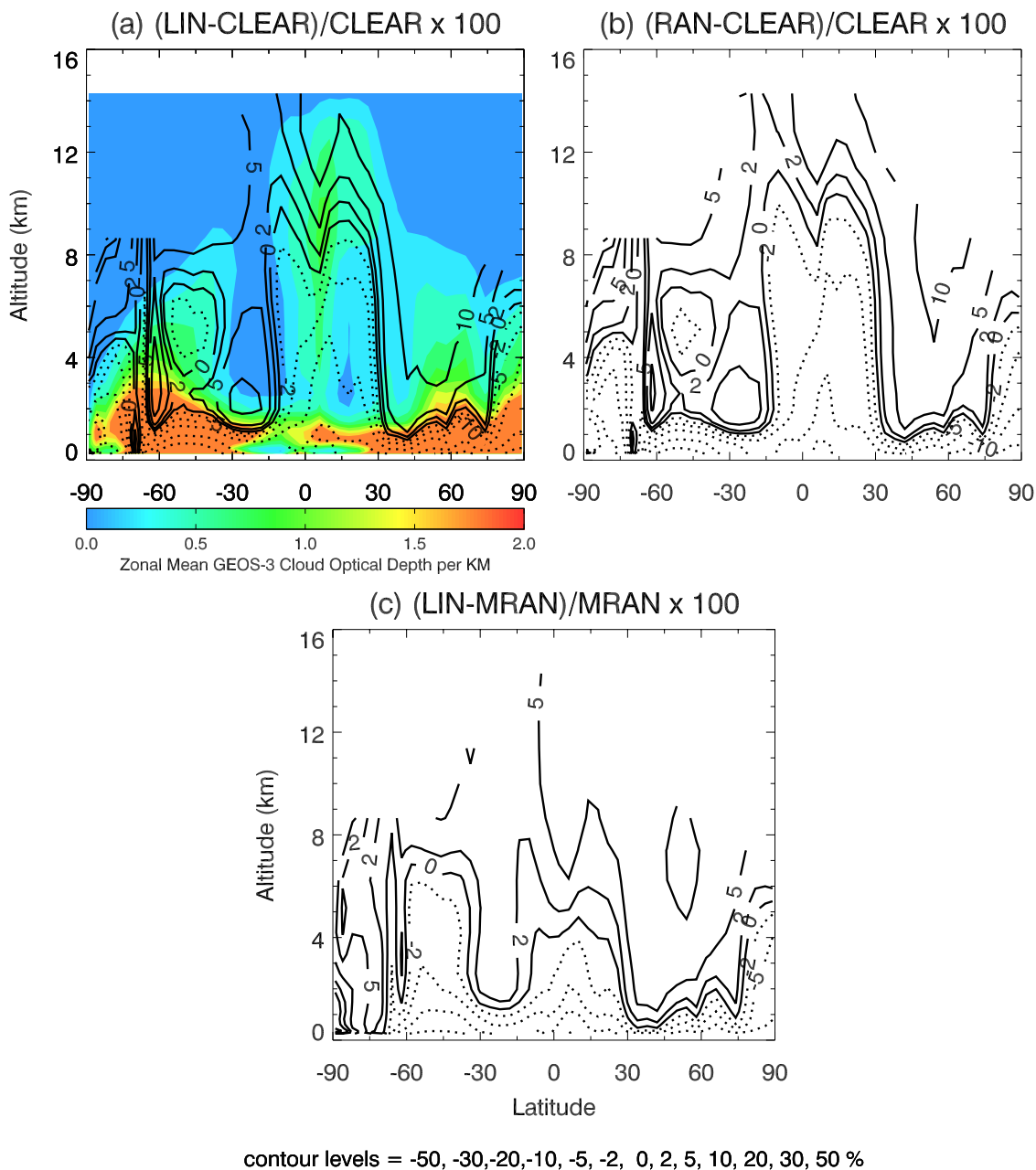


**Figure 10.** (a–c) Same as Figures 8a–8c but for OH.

concentrations that are close (within 5%) to those given by MRAN (not shown).

[38] Figure 11a shows the percentage changes in monthly zonal mean  $O_3$  due to the radiative effect of clouds (MRAN) in June 2001. The maximum impact on  $O_3$  ( $\sim 5\%$ ) is seen in the tropical upper troposphere with less than a few percent impact elsewhere. Contrasting with OH enhancements above clouds and reductions below clouds,  $O_3$  enhancements are found in most of the troposphere, partly reflecting the short lifetime of OH (seconds) and relatively long lifetime of  $O_3$  in the troposphere (days to a few weeks). The lower troposphere in the tropics and SH are overall a

regime of net  $O_3$  loss due to low  $NO_x$  environments (not shown). We find that the presence of tropical deep convective clouds suppresses this net  $O_3$  loss, thus increasing  $O_3$  concentrations in this part of the troposphere. The maximum positive percentage changes (up to  $\sim 20\text{--}30\%$ ) in surface  $O_3$  occur in the tropics (not shown), but large relative changes are usually associated with low ozone, resulting in small relative changes in zonal mean concentrations.

[39] Figure 11b shows the percentage changes in monthly zonal mean CO due to the radiative effect of clouds (MRAN) in June 2001. Cloud overlap has little effect. The overall impact of clouds on CO is not significant,

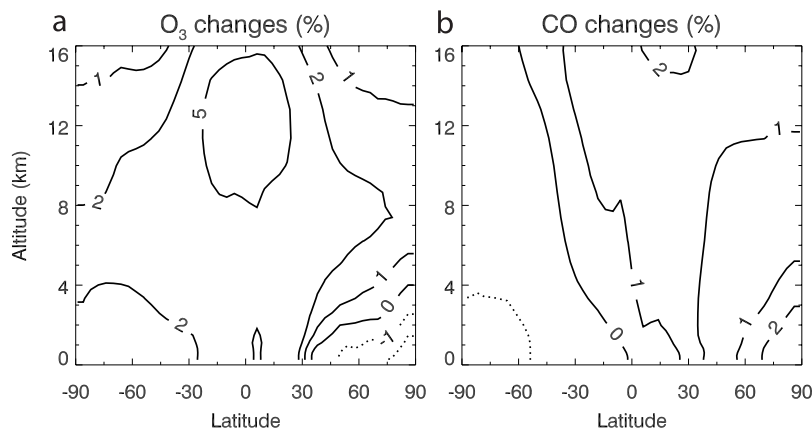


**Figure 11.** Simulated percentage changes in monthly zonal mean (a)  $\text{O}_3$  and (b) CO concentrations due to the radiative effect of clouds with the maximum-random cloud overlap assumption for June 2001.

although NH (SH) tends to see positive (negative) changes. The small changes in CO may be due to the fact that loss of CO by OH is partly compensated by CO production from hydrocarbons. The positive (negative) changes in NH (SH) reflect the fact that CO sources are dominated by direct emissions in continental source regions in NH but by OH oxidation of hydrocarbons in SH.

### 6.3. Comparison With Previous Modeling

[40] We compare here our model calculations with those of *Tie et al.* [2003]. There are some similarities. Both this study and that of *Tie et al.* [2003] found  $\text{O}_3$  enhancements in most of the troposphere due to the radiative effect of clouds, but the latter indicated much larger enhancements of  $\text{O}_3$  in the tropics with a maximum impact of  $\sim 20\text{--}30\%$  in the upper troposphere (see their Figure 14). When LIN or RAN rather than MRAN is used in our model, neither do we see significantly larger impact on  $\text{O}_3$ . It appears that the sensitivities of  $\text{O}_3$  to clouds in the two models, as they now stand, are quite different. Both studies found that using LIN and MRAN schemes have important effects on the calculation of the cloud effects, consistent with the study of *Feng et al.* [2004].

[41] There are more discrepancies between the two model calculations. Also shown in Table 2 are the MOZART-2 simulated percentage changes in the global tropospheric mean concentrations of key oxidants and global mean photolysis frequencies due to the radiative effect of clouds, as reported by *Tie et al.* [2003, 2006]. The small changes in global means found in this study are in distinct contrast with the large percentage changes (except for  $\text{NO}_x$ ) found in the MOZART-2 model [*Tie et al.*, 2003], in particular for OH (Table 2). *Tie et al.* [2003] reported a very similar  $\text{CH}_4$  lifetime (11.4 years) under clear-sky condition but significantly different  $\text{CH}_4$  lifetimes of  $\sim 5\text{--}6$  years (LIN) and  $\sim 8\text{--}9$  years (MRAN) under cloudy-sky conditions. Such dramatic changes in  $\text{CH}_4$  lifetime ( $-18\%$  to  $-46\%$ ) due to the presence of clouds or the use of different cloud overlap schemes are not seen in our model. There are some factors that may contribute to all these differences. First, we use mass-weighted method to calculate the global mean changes in tropospheric chemical species, while those reported by *Tie et al.* [2003] are based on the volume mixing ratios

averaged over each grid box below 200 mbar (X. Tie, personal communication, 2004). The non-mass-weighted method tends to give global mean concentrations erroneously weighted toward the middle and upper troposphere. Even if we calculate global mean changes in the same way as *Tie et al.* [2003] did, we do not find large percentage changes, only reflecting the offsetting effect of above-cloud enhancements and below-cloud reductions in our model. Second, the cloud vertical distributions in this study appear significantly different than those of *Tie et al.* [2003]. The MOZART-2 model uses online calculated cloud distribution with a high temporal resolution (20 min time interval). As pointed out by *Tie et al.* [2003], MOZART-2 tends to underestimate high cloud water in the tropics (see their Figure 8) where our model has more high cloud water (by a factor of 2–3). Both models have low cloud water of similar magnitude, including in the tropics (not shown). Relative to our model, MOZART-2 may therefore overestimate the reflection of solar radiation from tropical low clouds. However, our sensitivity experiments suggest that different cloud vertical distributions cannot explain the major discrepancies between the two model calculations (H. Liu et al., Sensitivity of tropospheric chemistry simulations to cloud vertical distributions and optical properties, manuscript in preparation, 2006; hereinafter referred to as Liu et al., manuscript in preparation, 2006). At present, to compare the two studies in a systematic way is beyond the scope of this study.

## 7. Discussion

[42] It is well established that tropospheric  $\text{O}_3$  is an important greenhouse gas, in particular in the upper troposphere. Because cloud optical properties may change because of anthropogenic influences through aerosol-cloud interactions, the sensitivity of tropospheric  $\text{O}_3$  is an important issue for assessment of anthropogenic perturbations to the climate. The reason for the different sensitivities of tropical upper tropospheric  $\text{O}_3$  to clouds in GEOS-CHEM (this work) and MOZART-2 [*Tie et al.*, 2003] is not immediately clear. It appears that global distributions of clouds are similar in the two models, except in the tropics where the optical depth due to high clouds tends to be

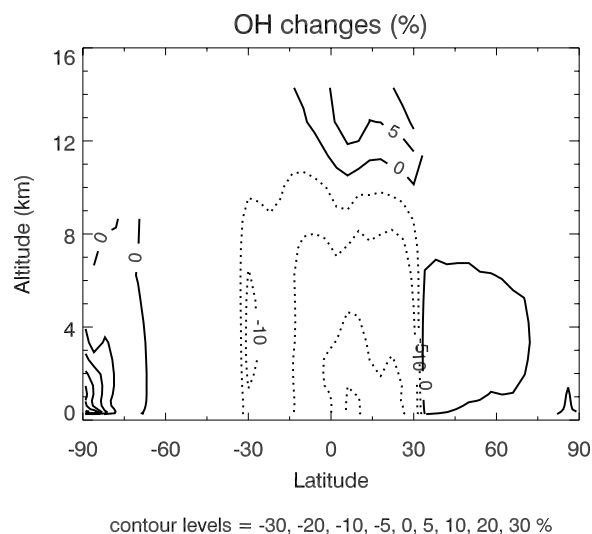


**Figure 12.** Simulated percentage changes in monthly zonal mean OH concentrations due to the radiative effect of tropical mid and high clouds ( $30^{\circ}\text{S}$ – $30^{\circ}\text{N}$ ) for June 2001, as reflected by subtraction of the simulation without tropical mid and high clouds from the simulation with global clouds. The linear assumption (LIN) is used.

underestimated in MOZART-2 [Tie *et al.*, 2003]. We conducted a sensitivity simulation using GEOS-CHEM where the GEOS-3 clouds in the tropical middle and upper troposphere were removed. The results do not indicate a larger effect of clouds on  $\text{O}_3$  either. It is also difficult to see how the different sensitivities might result from differences in the chemical mechanisms used in the two models. The global budget analysis of tropospheric  $\text{O}_3$  in MOZART-2 suggests that its tropospheric chemistry is not significantly more active than that of other global models [Horowitz *et al.*, 2003]. We argue that a  $\sim 20$ – $30\%$  increase in tropical upper tropospheric  $\text{O}_3$  solely due to the radiative effect of clouds is too large.

[43] Cloud treatments and diagnostics are still the major uncertainty in climate models, as reflected by the discrepancies in the cloud optical and physical properties from various meteorological archives. These cloud fields may affect the simulation of the tropospheric chemistry system. For instance, the meteorological fields driving the GEOS-CHEM model include a series of archives from GEOS DAS, i.e., GEOS-1, GEOS1-STRAT, GEOS-3 (this study), and GEOS-4. The global average cloud optical depths in GEOS-1 and GEOS1-STRAT appear to be a factor of 4–5 smaller than those in GEOS-3 (not shown). Cloud optical depths in GEOS-4 seem too low in the tropics when compared to GEOS-3 as well as MODIS and ISCCP satellite retrieval products, reflecting the optically much thinner clouds in the tropical middle and upper troposphere in GEOS-4 (not shown). The differences between the sensitivity simulation mentioned above (where the clouds in the tropical middle and upper troposphere were removed) and the standard simulation give us a sense of the impact of GEOS-3 and GEOS-4 cloud optical depth differences on the simulation of tropospheric chemistry. It suggests that using GEOS-4 cloud optical depths may overestimate OH concentrations by about 10–20% in most of the tropical troposphere (Figure 12), if LIN is used. Indeed, a recent

GEOS-CHEM full chemistry simulation driven by GEOS-4 showed significantly higher global OH concentrations than earlier simulations driven by GEOS-3 (J. Logan, personal communication, 2004). We will document in a separate paper the sensitivity of tropospheric chemistry simulations to cloud vertical distributions and optical properties (Liu *et al.*, manuscript in preparation, 2006). We suggest that the radiative effect of clouds on the simulation of tropospheric chemistry be assessed in the Global Modeling Initiative (GMI) framework [Douglass *et al.*, 1999] where the cloud fields from various meteorological archives can be utilized.

[44] With respect to the effect of cloud overlap on photochemistry, we improve over the study of Feng *et al.* [2004] in at least two aspects. First, we coupled the Fast-J radiative transfer model with GEOS-CHEM, while Feng *et al.* [2004] calculated photolysis frequencies with a linear or quasi-linear interpolation from a table of calculated photolysis frequencies for specified clear or cloudy conditions. They reported the global average errors in the cloudy-sky look-up table photolysis frequencies  $\text{J}[\text{O}^1\text{D}]$  and  $\text{J}[\text{NO}_2]$  are between  $-6\%$  and  $+1\%$  when compared to the exact method. These errors are on the order of the difference between RAN and MRAN (Figures 8 and 9) and therefore are relatively large. As our results have shown, the differences of photolysis frequencies above clouds or in the upper portion of clouds between using RAN and MRAN should be smaller than those between using LIN and MRAN, since LIN allows less solar radiation to penetrate down below the cloud. However, the results of Feng *et al.* [2004] seemed to show the former is larger than the latter for  $\text{J}[\text{O}^1\text{D}]$  in the tropics (see their Figure 7), reflecting the relatively large errors due to parameterized calculation of photolysis rates in their table look-up scheme. This suggests the importance of coupling the radiative transfer model with CTMs. Second, we included the full  $\text{O}_3$ - $\text{NO}_x$ - $\text{CO}$ - $\text{VOC}$  chemistry in our simulations while Feng *et al.* [2004] used prescribed concentrations of  $\text{O}_3$ ,  $\text{NO}_x$ ,  $\text{CO}$  and other long-lived species.

Our simulated effect of cloud overlap on OH should therefore be more consistent with the effect of clouds on other trace species.

[45] Cloud overlap assumptions used in the model have a significant influence on the calculated total cloud cover and radiation fields [Morcrette and Jakob, 2000; Bergman and Rasch, 2002; Stephens et al., 2004]. Observational studies however did not prefer any of the cloud assumptions (see the review of Feng et al. [2004]). In fact, existing overlap assumptions have significant limitations that may lead to unrealistic cloud distributions [Bergman and Rasch, 2002; Stephens et al., 2004]. For instance, Stephens et al. [2004] demonstrated that the random and maximum-random overlap methods create a vertical-resolution-dependent bias in model total cloudiness and radiative fluxes. Since GEOS-CHEM is an offline model, we do not include in our calculation the impact of cloud overlap on radiation fields of the atmosphere, nor do we try to examine which cloud overlap assumption gives better total cloudiness and surface and top-of-the-atmosphere radiation fluxes. We suggest using online CTMs to address the issue. On the other hand, current satellite observations of global cloudiness also suffer from multilayered cloud systems because of its assumption that only a single cloud layer is present in a given pixel. The potential for using satellites to detect cloud overlap however is encouraging [Pavolonis and Heidinger, 2004].

## 8. Summary and Conclusions

[46] We have used a state-of-the-art global 3-D model of tropospheric chemistry driven by assimilated meteorological data (GEOS-3) coupled with the Fast-J radiative transfer model [Wild et al., 2000] to assess the radiative effect of clouds on photolysis frequencies and key oxidants in the troposphere during 2001. Our aim was to improve our quantitative understanding of this effect on a global scale, including the associated uncertainties due to different cloud overlap assumptions. Three different methods are used to assess the impact of clouds on radiative transfer and they are the uniform cloud distribution method (linear assumption or LIN), an approximate random overlap assumption (RAN), and the maximum-random overlap assumption (MRAN).

[47] To properly take into account the radiative effect of clouds, we have evaluated GEOS-3 column cloud optical depth and cloud fraction with MODIS and ISCCP satellite retrieval products. We showed that MODIS and ISCCP monthly mean cloud optical depths (linear averages of pixel values) are actually comparable in magnitude. GEOS-3 cloud optical depths show peaks in the tropics associated with deep convective clouds and at midlatitudes associated with extratropical cyclones in NH and marine stratiform clouds in SH. These features reasonably agree with MODIS and ISCCP cloud retrieval products, although GEOS-3 tends to overestimate cloud optical depths in the tropics and SH midlatitudes. GEOS-3 cloud fraction agrees with MODIS and ISCCP products but appears lower at midlatitudes.

[48] While we have been able to reproduce with Fast-J the one-dimensional test cases for the radiative effect of clouds on photolysis rates in the literature, our online simulation results of the global impact of clouds on photolysis frequencies are significantly different than those of previous

studies in many aspects. Our calculation shows that globally averaged photolysis frequencies  $J[\text{O}^1\text{D}]$ ,  $J[\text{NO}_2]$  and  $J[\text{CH}_2\text{O}]$  in the troposphere are reduced by only  $\sim 2\text{--}4\%$  because of the impact of clouds with the use of any of the cloud overlap assumptions, reflecting an offsetting effect of above-cloud enhancements due to reflection of solar radiation and below-cloud reductions. This small global average effect and insensitivity to cloud overlap are in distinct contrast with a global modeling study using MOZART-2 [Tie et al., 2003] where a global average enhancement of 13% ( $\sim 45\text{--}62\%$ ) was found using MRAN (LIN). Despite the insensitivity of the global average effect to cloud overlap, we do find that LIN significantly overestimates the above-cloud enhancements and the below-cloud reductions when compared to RAN or MRAN, consistent with the findings of Feng et al. [2004]. However, our calculated differences in photolysis frequencies between LIN, RAN or MRAN are more consistent with these cloud overlap schemes themselves.

[49] Consistent with the previous studies [Tie et al., 2003; Feng et al., 2004], our calculations indicate that clouds have important effects on tropospheric chemistry through modification of photolysis frequencies. However, our results highlight that the dominant radiative effect of clouds is to influence the vertical redistribution of the intensity of photochemical activity while the global average effect remains modest. This contrasts with the result of Tie et al. [2003]. Differing vertical distributions of clouds may explain part, but not majority, of the discrepancies between models.

[50] Specifically, our calculated global mean changes in OH,  $\text{O}_3$ ,  $\text{NO}_x$ ,  $\text{HO}_2$ ,  $\text{CH}_2\text{O}$ , and CO due to clouds are generally less than 6% using any of the cloud overlap assumptions. For OH, the global mean change is insignificant ( $\sim 1\%$ ) but it shows much larger changes above (5–10%) and below (–5–20%) the tropical deep convective clouds and the midlatitude low-level clouds, as well as near the surface (approximately –20%). The global mean lifetime of  $\text{CH}_3\text{CCl}_3$  ( $\text{CH}_4$ ) increases by  $\sim 3\text{--}5\%$  from a clear-sky value of 6.5 (11) years; the positive impact of clouds reflects the fact that the lifetime of  $\text{CH}_3\text{CCl}_3$  ( $\text{CH}_4$ ) is more sensitive to OH in the lower troposphere where clouds strongly decrease OH concentrations. For  $\text{O}_3$ , the global mean effect is about 3–5% increase.  $\text{O}_3$  increases occur in most of the troposphere with maximum in the tropical upper troposphere, consistent with Tie et al. [2003]. Our calculated  $\text{O}_3$  increase in the tropical upper troposphere ( $\sim 5\text{--}8\%$ ) is however substantially smaller than that ( $\sim 20\text{--}30\%$ ) of Tie et al. [2003]. While  $\text{O}_3$  increases above the clouds in our model reflect the increased net  $\text{O}_3$  production due to backscattering of solar radiation,  $\text{O}_3$  increases below the tropical deep clouds and the SH marine stratus are a result of reduced net  $\text{O}_3$  losses in these regimes. The radiative effect of clouds on CO is not significant both globally and regionally in the vertical ( $\sim 1\text{--}2\%$ ), reflecting that loss of CO by OH is partly compensated by CO production from hydrocarbons.

[51] Our model results using different cloud overlap assumptions do not indicate which assumption is preferred, although one may argue that MRAN is more realistic. Relative to MRAN, LIN significantly overestimates the impact of clouds on tropospheric chemistry. We find that

RAN ( $\tau'_c = \tau_c \cdot f^{3/2}$ ) is a good approximation of MRAN in terms of the radiative impact of clouds on tropospheric chemistry. Since RAN is computationally much cheaper than MRAN, RAN is a good compromise between including the effect of cloud overlap and achieving computational efficiency.

[52] The radiative effect of clouds on tropospheric chemistry in a global CTM critically depends on the cloud optical properties and, in particular, on the vertical distribution of cloud optical depth and cloud fraction, which is still one of the largest uncertainties in current general circulation models and other meteorological products. For instance, there are important differences between the vertical distributions of cloud optical depth in the GEOS-3 and GEOS-4 meteorological archives, leading to significant differences in the simulated OH (oxidation capability) in the troposphere. Assimilating satellite observations of cloud optical properties in global models may help reduce such uncertainties. In particular, with the launchings of CALIPSO and CloudSat, a unique data set of cloud optical and physical properties as well as their vertical distribution will substantially improve our constraints on the radiative effect of clouds on tropospheric chemistry and climate. Eventually it will lead us to an improved understanding of cloud-chemistry-climate interactions in a changing climate.

[53] **Acknowledgments.** This research was supported by NASA Langley Research Center. We would like to thank William Rossow, Patrick Minnis and Paul Hubanks for useful suggestions; Joyce Penner, Daniel Jacob and three anonymous reviewers for helpful comments; Lawrence Takacs and Man-Li Wu for helping us understand the GEOS-3 archive; and Oliver Wild for discussions about Fast-J. MODIS and ISCCP products are distributed by NASA Goddard Distributed Active Archive Center and Langley Atmospheric Sciences Data Center, respectively. The GEOS-CHEM model is managed by the Atmospheric Chemistry Modeling Group at Harvard University with support from the NASA Atmospheric Chemistry Modeling and Analysis Program (ACMAP).

## References

- Allen, D. J., R. B. Rood, A. M. Thompson, and R. D. Hudson (1996), Three-dimensional radon 222 calculations using assimilated meteorological data and a convective mixing algorithm, *J. Geophys. Res.*, *101*, 6871–6881.
- Bergman, J. W., and P. J. Rasch (2002), Parameterizing vertically coherent cloud distributions, *J. Atmos. Sci.*, *59*, 2165–2182.
- Berntsen, T. K., and I. S. A. Isaksen (1997), A global three-dimensional chemical transport model for the troposphere: 1. Model description and CO and ozone results, *J. Geophys. Res.*, *102*, 21,239–21,280.
- Bey, I., D. J. Jacob, R. M. Yantosca, J. A. Logan, B. Field, A. M. Fiore, Q. Li, H. Liu, L. J. Mickley, and M. Schultz (2001a), Global modeling of tropospheric chemistry with assimilated meteorology: Model description and evaluation, *J. Geophys. Res.*, *106*, 23,073–23,096.
- Bey, I., D. J. Jacob, J. A. Logan, and R. M. Yantosca (2001b), Asian chemical outflow to the Pacific: Origins, pathways and budgets, *J. Geophys. Res.*, *106*, 23,097–23,114.
- Brasseur, G. P., D. A. Hauglustaine, S. Walters, P. J. Rasch, J.-F. Muller, C. Granier, and X. Tie (1998), MOZART, a global chemical tracer model for ozone and related chemical tracers: 1. Model description, *J. Geophys. Res.*, *103*, 28,265–28,289.
- Briegleb, B. P. (1992), Delta-Eddington approximation for solar radiation in the NCAR Community Climate Model, *J. Geophys. Res.*, *97*, 7603–7612.
- Cess, R. D., et al. (1996), Cloud feedback in atmospheric general circulation models: An update, *J. Geophys. Res.*, *101*, 12,791–12,794.
- Chandra, S., J. R. Ziemke, and R. V. Martin (2003), Tropospheric ozone at tropical and middle latitudes derived from TOMS/MLS residual: Comparison with a global model, *J. Geophys. Res.*, *108*(D9), 4291, doi:10.1029/2002JD002912.
- Collins, W. D. (2001), Parameterization of generalized cloud overlap for radiative calculations in general circulation models, *J. Atmos. Sci.*, *58*, 3224–3242.
- Crawford, J. H., D. Davis, G. Chen, R. Shetter, M. Muller, J. Barrick, and J. Olson (1999), An assessment of cloud effects on photolysis rates: Comparison of experimental and theoretical values, *J. Geophys. Res.*, *104*, 5725–5734.
- Dougllass, A. R., M. J. Prather, T. M. Hall, S. E. Strahan, P. J. Rasch, L. C. Sparling, L. Coy, and J. M. Rodriguez (1999), Choosing meteorological input for the global modeling initiative assessment of high-speed aircraft, *J. Geophys. Res.*, *104*, 27,545–27,564.
- Duncan, B. N., R. V. Martin, A. C. Staudt, R. Yevich, and J. A. Logan (2003), Interannual and seasonal variability of biomass burning emissions constrained by satellite observations, *J. Geophys. Res.*, *108*(D2), 4100, doi:10.1029/2002JD002378.
- Feng, Y., J. E. Penner, S. Sillman, and X. Liu (2004), Effects of cloud overlap in photochemical models, *J. Geophys. Res.*, *109*, D04310, doi:10.1029/2003JD004040.
- Fiore, A. M., D. J. Jacob, I. Bey, R. M. Yantosca, B. D. Field, A. C. Fusco, and J. G. Wilkinson (2002a), Background ozone over the United States in summer: Origin, trend, and contribution to pollution episodes, *J. Geophys. Res.*, *107*(D15), 4275, doi:10.1029/2001JD000982.
- Fiore, A. M., D. J. Jacob, B. D. Field, D. G. Streets, S. D. Fernandes, and C. Jang (2002b), Linking ozone pollution and climate change: The case for controlling methane, *Geophys. Res. Lett.*, *29*(19), 1919, doi:10.1029/2002GL015601.
- Fiore, A. M., D. J. Jacob, R. Mathur, and R. V. Martin (2003a), Application of empirical orthogonal functions to evaluate ozone simulations with regional and global models, *J. Geophys. Res.*, *108*(D14), 4431, doi:10.1029/2002JD003151.
- Fiore, A. M., D. J. Jacob, H. Liu, R. M. Yantosca, T. D. Fairlie, and Q. Li (2003b), Variability in surface ozone background over the United States: Implications for air quality policy, *J. Geophys. Res.*, *108*(D24), 4787, doi:10.1029/2003JD003855.
- Geleyn, J. F., and A. Hollingsworth (1979), An economical analytical method for the computation of the interaction between scattering and line absorption of radiation, *Contrib. Atmos. Phys.*, *52*, 1–16.
- Hartmann, D. L., et al. (1999), Radiation, clouds, water vapor, precipitation, and atmospheric circulation, in *EOS Science Plan: The State of Science in the EOS Program*, edited by M. D. King, chap. 2, NASA, NP-1998-12-069-GSFC, 39–114.
- Herman, J. R., and E. A. Celarier (1997), Earth surface reflectivity climatology at 340–380 nm from TOMS data, *J. Geophys. Res.*, *102*, 28,003–28,011.
- Hogan, R. J., and A. J. Illingworth (2000), Deriving cloud overlap statistics from radar observations, *Q. J. R. Meteorol. Soc.*, *126*, 1–7.
- Horowitz, L. W., et al. (2003), A global simulation of tropospheric ozone and related tracers: Description and evaluation of MOZART, version 2, *J. Geophys. Res.*, *108*(D24), 4784, doi:10.1029/2002JD002853.
- Houghton, J. T., Y. Ding, D. J. Griggs, M. Noguer, P. J. van der Linden, and D. Xiaosu (Eds.) (2001), *Climate Change 2001: The Scientific Basis*, 944 pp., Cambridge Univ. Press, New York.
- Jacob, D. J. (2000), Heterogeneous chemistry and tropospheric ozone, *Atmos. Environ.*, *34*, 2131–2159.
- Jacob, D. J., E. W. Gottlieb, and M. J. Prather (1989), Chemistry of a polluted cloudy boundary layer, *J. Geophys. Res.*, *94*, 12,975–13,002.
- Junkermann, W. (1994), Measurements of the J(O<sup>1</sup>D) actinic flux within and above stratiform clouds and above snow surfaces, *Geophys. Res. Lett.*, *21*, 793–796.
- Landgraf, J., and P. J. Crutzen (1998), An efficient method for online calculations of photolysis and heating rates, *J. Atmos. Sci.*, *55*, 863–878.
- Lefer, B. L., R. E. Shetter, S. R. Hall, J. H. Crawford, and J. R. Olson (2003), Impact of clouds and aerosols on photolysis frequencies and photochemistry during TRACE-P: 1. Analysis using radiative transfer and photochemical box models, *J. Geophys. Res.*, *108*(D21), 8821, doi:10.1029/2002JD003171.
- Li, Q., et al. (2001), A tropospheric ozone maximum over the Middle East, *Geophys. Res. Lett.*, *28*, 3235–3238.
- Li, Q., D. J. Jacob, T. D. Fairlie, H. Liu, R. V. Martin, and R. M. Yantosca (2002a), Stratospheric versus pollution influences on ozone at Bermuda: Reconciling past analyses, *J. Geophys. Res.*, *107*(D22), 4611, doi:10.1029/2002JD002138.
- Li, Q., et al. (2002b), Transatlantic transport of pollution and its effects on surface ozone in Europe and North America, *J. Geophys. Res.*, *107*(D13), 4166, doi:10.1029/2001JD001422.
- Liang, X.-Z., and W.-C. Wang (1997), Cloud overlap effects on general circulation model climate simulations, *J. Geophys. Res.*, *102*(D10), 11,039–11,047.
- Lin, S.-J., and R. B. Rood (1996), Multidimensional flux-form semi-Lagrangian transport schemes, *Mon. Weather Rev.*, *124*, 2046–2070.
- Liu, H., D. J. Jacob, I. Bey, and R. M. Yantosca (2001), Constraints from <sup>210</sup>Pb and <sup>7</sup>Be on wet deposition and transport in a global three-dimensional chemical tracer model driven by assimilated meteorological fields, *J. Geophys. Res.*, *106*, 12,109–12,128.

- Liu, H., D. J. Jacob, L. Y. Chan, S. J. Oltmans, I. Bey, R. M. Yantosca, J. M. Harris, B. N. Duncan, and R. V. Martin (2002), Sources of tropospheric ozone along the Asian Pacific Rim: An analysis of ozonesonde observations, *J. Geophys. Res.*, *107*(D21), 4573, doi:10.1029/2001JD002005.
- Liu, H., D. J. Jacob, J. E. Dibb, A. M. Fiore, and R. M. Yantosca (2004), Constraints on the sources of tropospheric ozone from  $^{210}\text{Pb}$ - $^7\text{Be}$ -ozone correlations, *J. Geophys. Res.*, *109*, D07306, doi:10.1029/2003JD003988.
- Mao, H., W.-C. Wang, X.-Z. Liang, and R. W. Talbot (2003), Global and seasonal variations of  $\text{O}_3$  and  $\text{NO}_2$  photodissociation rate coefficients, *J. Geophys. Res.*, *108*(D7), 4216, doi:10.1029/2002JD002760.
- Martin, R. V., et al. (2002), Interpretation of TOMS observations of tropical tropospheric ozone with a global model and in situ observations, *J. Geophys. Res.*, *107*(D18), 4351, doi:10.1029/2001JD001480.
- McLinden, C. A., S. C. Olsen, B. Hannegan, O. Wild, M. J. Prather, and J. Sundet (2000), Stratospheric ozone in 3-D models: A simple chemistry and the cross-tropopause flux, *J. Geophys. Res.*, *105*, 14,653–14,665.
- Morcrette, J.-J., and C. Jakob (2000), The response of the ECMWF model to changes in the cloud overlap assumption, *Mon. Weather Rev.*, *128*, 1707–1732.
- Olson, J., et al. (1997), Results from the Intergovernmental Panel on Climatic Change Photochemical Model Intercomparison (PhotoComp), *J. Geophys. Res.*, *102*, 5979–5991.
- Park, R. J., D. J. Jacob, B. D. Field, R. M. Yantosca, and M. Chin (2004), Natural and transboundary pollution influences on sulfate-nitrate-ammonium aerosols in the United States: Implications for policy, *J. Geophys. Res.*, *109*, D15204, doi:10.1029/2003JD004473.
- Pavolonis, M. J., and A. K. Heidinger (2004), Daytime cloud overlap detection from AVHRR and VIIRS, *J. Appl. Meteorol.*, *43*, 762–778.
- Penner, J. E., C. S. Atherton, J. Dignon, S. J. Ghan, J. J. Walton, and S. Hameed (1991), Tropospheric nitrogen: A three-dimensional study of sources, distributions, and deposition, *J. Geophys. Res.*, *96*, 959–990.
- Pickering, K. E., et al. (1998), Vertical distributions of lightning  $\text{NO}_x$  for use in regional and global chemical transport models, *J. Geophys. Res.*, *103*(D23), 31,203–31,216.
- Pinker, R., H. Wang, M. King, and S. Platnick (2003), First use of MODIS data to cross-calibrate with GEWEX/SRB data sets, *GEWEX News*, *13*(4), 4–5.
- Platnick, S., M. D. King, S. A. Ackerman, W. P. Menzel, B. A. Baum, J. C. Riedi, and R. A. Frey (2003), The MODIS cloud products: Algorithms and examples from Terra, *IEEE Trans. Geosci. Remote Sens.*, *41*(2), 459–473.
- Prather, M., and D. Jacob (1997), A persistent imbalance in  $\text{HO}_x$  and  $\text{NO}_x$  photochemistry of the upper troposphere driven by deep tropical convection, *Geophys. Res. Lett.*, *24*, 3189–3192.
- Prinn, R. G., et al. (2001), Evidence for substantial variations of atmospheric hydroxyl radicals in the past two decades, *Science*, *292*, 1882–1888.
- Rossow, W. B., and R. A. Schiffer (1999), Advances in understanding clouds from ISCCP, *Bull. Am. Meteorol. Soc.*, *80*, 2261–2287.
- Rossow, W. B., A. W. Walker, D. E. Beusichel, and M. D. Roiter (1996), International Satellite Cloud Climatology Project (ISCCP) documentation of new cloud datasets, Int. Council of Sci. Unions, Paris, Jan.
- Shindell, D. T., J. L. Grenfell, D. Rind, and V. Grewel (2001), Chemistry-climate interactions in the Goddard Institute for Space Studies general circulation model: 1. Tropospheric chemistry description and evaluation, *J. Geophys. Res.*, *106*, 8047–8075.
- Slingo, A., and H. Schrecker (1982), On the short-wave radiative properties of stratiform water clouds, *Q. J. R. Meteorol. Soc.*, *108*, 407–426.
- Spivakovsky, C. M., R. Yevich, J. A. Logan, S. C. Wofsy, and M. B. McElroy (1990), Tropospheric OH in a three-dimensional chemical tracer model: An assessment based on observations of  $\text{CH}_3\text{CCl}_3$ , *J. Geophys. Res.*, *95*, 18,441–18,471.
- Spivakovsky, C. M., et al. (2000), Three-dimensional climatological distribution of tropospheric OH: Update and evaluation, *J. Geophys. Res.*, *105*, 8931–8980.
- Stephens, G. L., N. B. Wood, and P. M. Gabriel (2004), An assessment of the parameterization of subgrid-scale cloud effects on radiative transfer. Part I: Vertical overlap, *J. Atmos. Sci.*, *61*, 715–732.
- Stubenrauch, C. J., A. D. Del Genio, and W. B. Rossow (1997), Implementation of subgrid cloud vertical structure inside a GCM and its effect on the radiation budget, *J. Clim.*, *10*, 273–287.
- Tang, Y., et al. (2003), Impacts of aerosols and clouds on photolysis frequencies and photochemistry during TRACE-P: 2. Three-dimensional study using a regional chemical transport model, *J. Geophys. Res.*, *108*(D21), 8822, doi:10.1029/2002JD003100.
- Thompson, A. M. (1984), The effect of clouds on photolysis rates and ozone formation in the unpolluted troposphere, *J. Geophys. Res.*, *89*, 1341–1349.
- Thompson, A. M., M. A. Huntley, and R. W. Stewart (1990), Perturbations of tropospheric oxidants, 1985–2035: Calculations of ozone and OH in chemically coherent regions, *J. Geophys. Res.*, *95*, 9829–9844.
- Tie, X., S. Madronich, S. Walters, R. Zhang, P. Rasch, and W. Collins (2003), Effect of clouds on photolysis and oxidants in the troposphere, *J. Geophys. Res.*, *108*(D20), 4642, doi:10.1029/2003JD003659.
- Tie, X., S. Madronich, S. Walters, R. Zhang, P. Rasch, and W. Collins (2006), Correction to “Effect of clouds on photolysis and oxidants in the troposphere,” submitted to *J. Geophys. Res.*
- Wild, O., X. Zhu, and M. J. Prather (2000), Fast-J: Accurate simulation of in- and below-cloud photolysis in tropospheric chemical models, *J. Atmos. Chem.*, *37*, 245–282.
- Yang, H., and H. Levy (2004), Sensitivity of photodissociation rate coefficients and  $\text{O}_3$  photochemical tendencies to aerosols and clouds, *J. Geophys. Res.*, *109*(D24), D24301, doi:10.1029/2004JD005032.
- G. Chen, J. H. Crawford, and R. B. Pierce, Mail Stop 401B, NASA Langley Research Center, Hampton, VA 23681, USA.
- M. J. Evans, School of Earth and the Environment, University of Leeds, Leeds LS2 9JT, UK.
- Y. Feng, Center for Atmospheric Sciences, Scripps Institution of Oceanography, University of California, San Diego, La Jolla, CA 92093, USA.
- C. Kittaka, Science Applications International Corporation, Hampton, VA 23681, USA.
- H. Liu, National Institute of Aerospace, 100 Exploration Way, Hampton, VA 23666-6147, USA. (hyl@nianet.org)
- J. A. Logan and R. M. Yantosca, Division of Engineering and Applied Sciences, Harvard University, 29 Oxford Street, Cambridge, MA 02138, USA.
- P. Norris, NASA Goddard Space Flight Center, Code 610, Greenbelt, MD 20771, USA.
- S. E. Platnick, NASA Goddard Space Flight Center, Code 613.2, Greenbelt, MD 20771, USA.
- X. Tie, National Center for Atmospheric Research, Boulder, CO 80307, USA.